SEPTEMBER 2017

U.PORTO
INSTITUTO DE CIÊNCIAS BIOMÉDICAS ABEL SALAZAR
UNIVERSIDADE DO PORTO

U.PORTO
FEUP FACULDADE DE ENGENHARIA
UNIVERSIDADE DO PORTO

Carcinoembryonic antigen targeted polymeric nanoparticles for drug delivery

INÊS SOUSA PEREIRA

DISSERTATION FOR THE DEGREE OF MASTER IN BIOENGINEERING AT THE FACULDADE DE ENGENHARIA DA UNIVERSIDADE DO PORTO AND INSITUTO DE CIÊNCIAS BIOMÉDICAS ABEL SALAZAR

Carcinoembryonic antigen targeted polymeric nanoparticles for drug delivery

Inês Sousa Pereira

DISSERTATION FOR THE DEGREE OF MASTER IN BIOENGINEERING AT THE FACULDADE DE ENGENHARIA DA UNIVERSIDADE DO PORTO AND INSITUTO DE CIÊNCIAS BIOMÉDICAS ABEL SALAZAR

Supervisor: Bruno Sarmento, PhD

September 2017

"Mil vezes venturosos os que a sorte
Na terra lusitana fez nascidos
Porque estes viverão além da morte
Por séculos felizes distinguidos."
José Coutinhas, in *Um Porto para o Mundo*

Acknowledgments

To my supervisor, Prof Bruno Sarmento, thank you for accepting me as a master student with open arms. I felt really welcomed in this group and inspired to continue a journey in research that is only starting. Thank you for all the guidance and specially thank you for all the patient and faith placed in me.

I would like to thank all the institutions, FEUP – Faculdade de Engenharia da Universidade do Porto, ICBAS – Instituto de Ciências Biomédicas Abel Salazar and i3S – Instituto de Investigação e Inovação em Saúde that accepted me and were crucial to the development of this work.

One of my biggest acknowledgements goes to all my teammates, especially the ones most close to me – Patrick, Anna, Christina, Andreia and Karla. Thank you for all the help given to me and for the friendship built. All of you were important for my growth this past months. A special acknowledgement to Flávia, thank you so much for all the help and patient you had with me, it was a pleasure working with you and I hope it is just the beginning. To Catarina and Mafalda, a special thank you, my fellow Master students, for all the support and understanding we shared!

Antónia e Amauri, my mentors in the arts. Even though yours contribute is not related to my scientific work, I must thank you too. Thank you for your support and for always believing in me.

To my childhood friends Sofia, Joana, Carina, Tânia, Claudia and Camila for keeping up with me all these years and for always being able to cheer me up. To Carolina, Carla and Sónia, my friends from Vila Real, thank you for all the support! To my classmates Débora and Ana and to Pedro, thank you for all the encouragement! You all mean a lot to me!

Lastly, an enormous thank you to my family. Without their support, I would certainly not be where I am today. To my mother, for never doubting my capacities and for encouraging me to be better every day. To my father that even away always asks me how my cells are. To my sister, for being my best friend and being there for me every time I needed. To my cousin Verónica, my aunt Marta and my grandmother Laura, thank you for your good mood and encouragement! Thank you!

List of contents

Abstract

Nanoparticles (NP) have been developed and studied for more than 20 years as drug delivery carriers. Particular attention has been focused on their exploitation for cancer treatment, as a mean to efficiently deliver the anti-cancer drugs to tumor-site, improving the outcome of those molecules. In this dissertation, polymeric poly(lactic-co-glycolic)-polyethyleneglicol (PLGA-PEG) nanoparticles were produced and surface-functionalized with an antibody targeting the Carcinoembryonic Antigen (CEA) of intestinal epithelial cells. CEA is overexpress in a number of cancers, including colorectal cancer. Nanoparticles were loaded with paclitaxel (PTX), an anti-cancer drug, and the most relevant physical-chemical properties regarding mean particle size, surface charge and drug loading were determined. The mean size and polydispersity index (PDI) of optimized formulation were round around 177 nm and 0.14, respectively. The surface charge was negative, close to -6 mV. Association efficacy and drug loading were measured though high performance liquid chromatography (HPLC) and were found to be 99% and 20%, respectively. Morphology of the nanoparticles was characterized using transmission electron microscopy (TEM), showing spherical structures. The release profile of PTX was assessed, confirming the sustain release up to 48 h. Cytotoxicity of the nanoparticles was evaluated though a MTT assay in two intestine epithelial carcinoma cell lines (Caco-2 clone and SW480), showing no cytotoxicity for nanoparticles, either unloaded or loaded with PTX. The functionalization of the particles was accomplished through the carbodiimide chemistry and its efficacy tested through an ELISA assay. Results confirmed the presence of the antibody on the surface of nanoparticles. Flow cytometry experiments were performed to confirm the targeting ability of functionalized nanoparticles to CEA expressing cells. Overall, surface-modified PLGA-PEG nanoparticles with an antibody targeting the CEA were successfully developed as nanocarriers for PTX and interacted with CEA expressing cells, being potentially used as targeted systems to treat colorectal cancer.

Resumo

As nanopartículas (NP) têm sido desenvolvidas e estudadas há mais de 20 anos como veículos de transporte de fármaco. Particularmente explorados para o tratamento de cancro, como um meio para uma entrega de fármaco anticancerígeno localizada no tumor, melhorando o efeito destas moléculas. Nesta dissertação, nanopartículas poliméricas de poly(lactic-co-glycolic)-polyethyleneglicol (PLGA-PEG) foram produzidas e a sua superfície funcionalizada com um anticorpo específico para o Carcinoembryonic Antigen (CEA) das células tumorais epiteliais intestinais. CEA é sobrexpresso em vários cancros, incluindo o cancro colorectal. Nas partículas foi encapsulado paclitaxel (PTX), um fármaco anticancerígeno, e as propriedades físico-químicas mais relevantes, nomeadamente o tamanho médio da partícula, carga da superfície e eficácia de encapsulação do fármaco foram determinadas. O tamanho médio e o índice de polidispesividade da formulação otimizada era por volta de 177 nm e 0.14, respetivamente. A carga da superfície era negativa, perto dos -6mV. A eficácia de associação e encapsulação do fármaco foram medidas através de cromatografia líquida de alta performance (HPLC) e foram 99% e 20%, respetivamente. A morfologia das nanopartículas foi caracterizada usando Microscopia Eletrónica de Transmissão (TEM), e mostrou estruturas esféricas e uniformes. O perfil de libertação de PTX foi avaliado, confirmando uma libertação controlada até 48h. A citotoxicidade das nanopartículas foi avaliada através de um ensaio de MTT em duas linhas celulares epiteliais de carcinoma intestinal (Caco-2 clone e SW480). Os resultados não mostraram citotoxicidade das nanopartículas, vazias ou com fármaco. A funcionalização das partículas foi feita usando a química carbodiimida e a sua eficácia foi testada através de um ensaio ELISA. A presença do anticorpo na superfície das nanopartículas foi confirmada nos resultados. Experiências de citometria de fluxo foram realizadas para confirmar a capacidade de target das partículas funcionalizadas nas células que expressavam CEA. Em geral, nanopartículas de PLGA-PEG modificadas na superfície com o anticorpo específico para CEA foram desenvolvidas com sucesso como veículos para o transporte de paclitaxel e provaram interagir com as células que expressam CEA, podendo ser potencialmente usadas como sistemas alvo para tratamento de cancro colorectal.

List of figures

List of tables

Abbreviations and symbols

Ab	Antibody
AE	Association Efficiency
ATCC	American type culture collection
BSA	Bovine serum albumin
CEA	Carcinoembryonic antigen
CEACAM	Carcinoembryonic antigen cell adhesion molecule
CRC	Colorectal cancer
Da	Dalton
DL	Drug Loading
DLS	Dynamic light scattering
DMEM	Dulbecco's modified eagle medium
DMSO	Dimethylsulfoxide
EDC	1-ethyl-3-(3-dimethylaminopropyl) carbodiimide
ELISA	Enzyme-linked immunosorbent assay
ELS	Electrophoretic light scattering
EMA	European medicines agency
EPR	Enhanced permeability and retention
FACS	Fluorescent-activated cell sorting
FBS	Fetal bovine serum
FDA	Food and drug administration
FU	Fluorescent unit
HPLC	High performance liquid chromatography
^{1}H NMR	Proton nuclear magnetic resonance
IC50	Minimal inhibitory concentration
mAb	Monoclonal antibody
MES	2-(N-morpholino) ethanesulfonic acid
MTT	3-(4,5,-dimethylthiazol-2-yl)-2,5-diphenyltetrazolium bromide
NaCl	Sodium chloride
NCI	National cancer institute
NEAA	Non-essential aminoacids
NHS	N-hydroxysuccinimide

NP	Nanoparticle
PBS	Phosphate buffered saline
PdI	Polydispersity index
PEG	Poly(ethyleneglycol)
PLGA	Poly(lactic-co-glycolic-acid)
PTX	Paclitaxel
PVA	Polyvinyl alcohol
R^2	Coefficient of determined value
RA	Radiofrequency ablation
SD	Standard deviation
STIR	Selective internal radiation therapy
TEM	Transmission electron microscopy
TMS	Tetramethylsilane
6-C	6-Coumarin

Chapter 1

1.1. Introduction

Colorectal cancer is one of the most diagnosed cancers worldwide (1). Despite diagnostic advances in the last years, most patient are only diagnosed in advanced stages, making this one of the most lethal oncologic diseases (2). Conventional treatments are not always efficient as they should since 50% of cases have recurrent disease (3). Thus, more efficient treatment should be addressed.

Paclitaxel (PTX) is one of the drugs used in the treatment of colorectal cancer. This drug, even highly efficient, is extremely hydrophobic, which difficult its solubility during the intravenous administration. A better pharmaceutical formulation to transport PTX to a target cancer would increase its therapeutic effect, improving the cancer treatment.

One of the most explored vehicles in drug delivery research are nanoparticles (4). These nanocarriers are capable to transport hydrophilic and hydrophobic drugs with a high loading capacity, enhancing the circulation time of the drug and its bioavailability, making them excellent for drug delivery (5). Another interesting characteristic of nanoparticles is the possibility of surface functionalization (6). A target moiety, for example an antibody, can be link to the surface and allow a specific bond between the particle and the target site.

For colorectal cancer, a target therapy would decrease the secondary effects of chemotherapy and improve the efficacy of the treatment (7). To do so, a specific receptor of intestine cancer cells can be the target used for these nanoparticles. One example of a receptor is carcinoembryonic antigen (CEA), which is found in the surface of several cancer cells, including colorectal cancer (8).

1.2. Objectives of this project

The production of polymeric nanoparticle with functionalized surface that allowed specific binding to colorectal cancer cells and capable of encapsulation paclitaxel and releasing it in a controlled manner, for an intravenous administration, was the mail goal of this work. To accomplish this goal, nanoparticles were produced and functionalized and the physical-chemical properties assessed, namely average size, size distribution, surface charge, association efficacy and drug loading. The *in vitro* release profile of the particles was evaluated as well. The cell studies involved a cytotoxicity assay to ensure the safety of the particles as well as cell-

nanoparticle interaction studies. These last studies, important to assess the target capacity of the system, had to be performed against a colorectal cell line positive for CEA expression, using a CEA negative control cell line.

1.3. Organization

This dissertation is organized in five chapters. **Chapter 1** gives a brief context, motivation and organization of the work. **Chapter 2** consists in a literature review of the main subjects of the dissertation. **Chapter 3** gives an overview of the materials a methodology and **Chapter 4** presents the results and discussion of them. **Chapter 5** presents the conclusion and future perspectives.

Chapter 2

2.1 Literature review

2.1.1 Colorectal cancer

Colorectal cancer (CRC) is one of the most serious cancer worldwide. Indeed it is the third most diagnosed cancer and the fourth most lethal (2). It was estimated in 2012 that 103,170 new cases appeared only in United States (9). In Portugal, colorectal cancer is the second most common in women and third in men (10). Age, personal and family history, racial and ethnic background are the main risk factors for developing this condition, as well as diet and lifestyle (11). Only a small percentage is due to genetic disorders (12). Colonoscopy remains the primary diagnosis method, and even though prevention screenings are recommended, only 50% of the Portuguese population apply them (10, 13).

Usually, this type of cancer starts in the lining of the bowel and then spreads to the musde layer underneath and finally to through the bowel wall (14). Stage zero is considered when the tumour is confined in the mucosa, also known as carcinoma *in situ*. In stage I, the tumour has invaded the inner layer of the mucosa. When the tumour has reached beyond the mucous layer, but not though lymph nodes metastasis, is considered to be on stage II. This stage is divided in three sections, A, B and C when the tumour reached the muscular layer, outermost layer or beyond colon, respectively. Stage III is characterized by the invasion colon wall and lymph nodes. This stage is also divided in three sections, section A is when tumour reached the inner layer of colon, B when reached the middle and C outer layer and surrounded nodes. When tumour is in stage IV, there are already metastases in distant organs, such as liver or ovary (**Figure 1**). Within the patients, only 39% are diagnosed when the cancer is in a local stage, giving them a 5-year rate survival of 90%. But this survival rate decreases to 71% for patients diagnosed with regional cancer and to 14% for the patients diagnosed with distant-stage cancer. The survival rate is very influenced by the different access to screening, treatment and prevalence of other diseases in the patients (1).

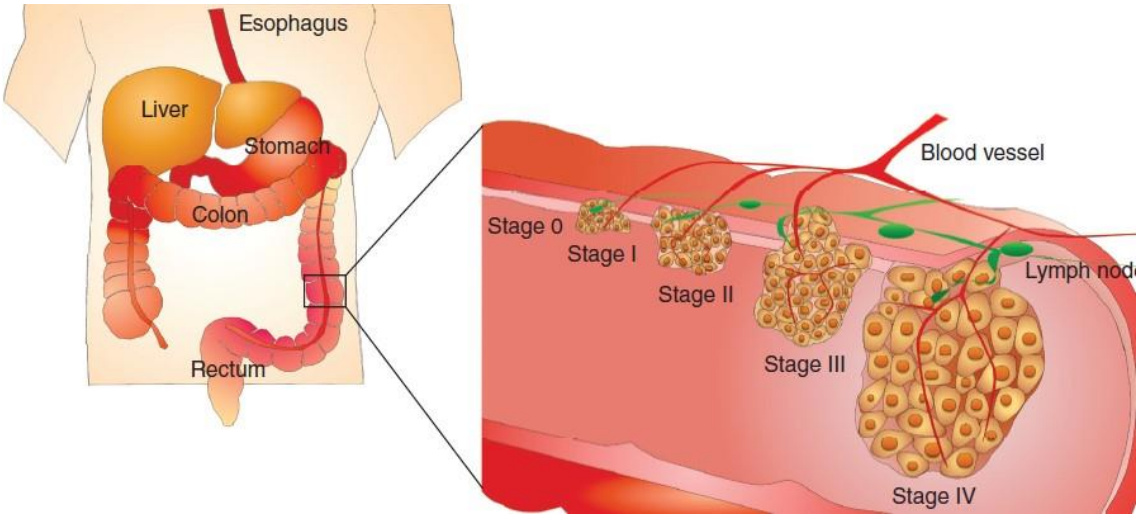

Fig. 1 *Colorectal tumour stages accordingly to the American Joint Committee on Cancer. Stage 0: the tumour is confined to the mucosa. Stage I: Tumour invades the inner layer of the mucosa. Stage II: tumour has spread through the colon (muscular layer, outermost layer or beyond), but without lymph node metastasis; Stage III: tumour has spread though colon (inner, middle or outer layer) and lymph nodes metastasis; Stage IV: tumour has metastasised in distant organs such as the liver. Adapted from (7).*

The most important frequent treatments used in colorectal cancer are polypectomy and surgery, radiotherapy and chemotherapy. Polypectomy is the removal of polyps during a colonoscopy and surgery remains the primary way to remove solid tumours. Patients with colon cancer in stage I and II usually undergo partial or total colectomy alone. Some cases in stage II and most cases in stage III undergo chemotherapy as well as colectomy, in order to decrease the recurrence disease. For rectal cancer patients, the most common treatment in stage I is proctectomy or proctocolectomy, some cases combined with radiotherapy and/or chemotherapy. In stage II or III, radiotherapy and chemotherapy is always applied after proctectomy or proctocolectomy (15). Usually these methods are combined with medication and radiotherapy and if the tumour is removed in the first stages, the patient might recover completely (9). Unfortunately not all the cases are noticeable at such initial stage and there is always the risk of post-surgical complication, especially in the elderly people (16). Radiotherapy uses ionizing radiation to control the proliferation of tumour cells. It can be classified in selective internal radiation therapy (SIRT), trans-arterial chemoembolization (TACE) and radiofrequence abalation (RA). This method is always associated with risks since radiation can induce d amages in normal cells (17). Chemotherapy is one of the most used methods to treat cancer. It is based on agents such as anti-metabolites (e.g. 5-fluorouracil), topoisomerase inhibitors (e.g.doxorubicin) or taxanes (e.g. paclitaxel) capable of kill malignant cells and stop the tumour growth. This type of drug interferes with DNA replication and chromosomal separation. One of the primary characteristics of CRC is its high cellular heterogeneity caused by biologic and genetic alterations, which leads to a grand variety between tumours (13). This variety makes the

chemotherapeutic agents not specific and even though they are highly effective, they lead to dose-limited side effects such as nausea, finger numbness, hair loss and fatigue (18, 19). The side effects of the treatment are noticeable even to cancer survivals. Chronic diarrhea, incontinence, bladder and sexual dysfunction are among the common health problems (15). Even though protocols have been followed that allowed the use of more than one chemotherapeutic agent in a series of cycles, the different concentrations on the plasma promote the development of drug resistance (20, 21). Surgical resection of the tumour and the conventional cancer treatments are not a cure insurance. Nearly 50% of colorectal carcinoma patients develop the disease once more (3). This recurrence rates combined with all the secondary effects of colorectal cancer therapy lead to the conclusion that better solutions should be implemented, using a more effective approach to treat this disease.

2.1.2 Paclitaxel

One of the most used chemoactive drugs is paclitaxel (PTX). PTX was first isolated in the beginning of the 1960s from the bark of Pacific Yew and its structure was published in 1971 (22). Being an important member of the taxanes in use today, this 853 Da drug with a molecular formula of $C_{47}H_{51}NO_{14}$ (**Figure 2**), interferes with microtubule function, causing hyperstability and dysfunction of the microtubules, leading to severe damage in the mitosis process leading to cell death. Considered one of the most significant advances in chemotherapy by the National Cancer Institute (NCI), PTX as a potent anti-tumour against a vast number of cancers such as breast, gastric, lung, esophageal, bladder, colon, ovarian or prostatic cancer (23, 24).

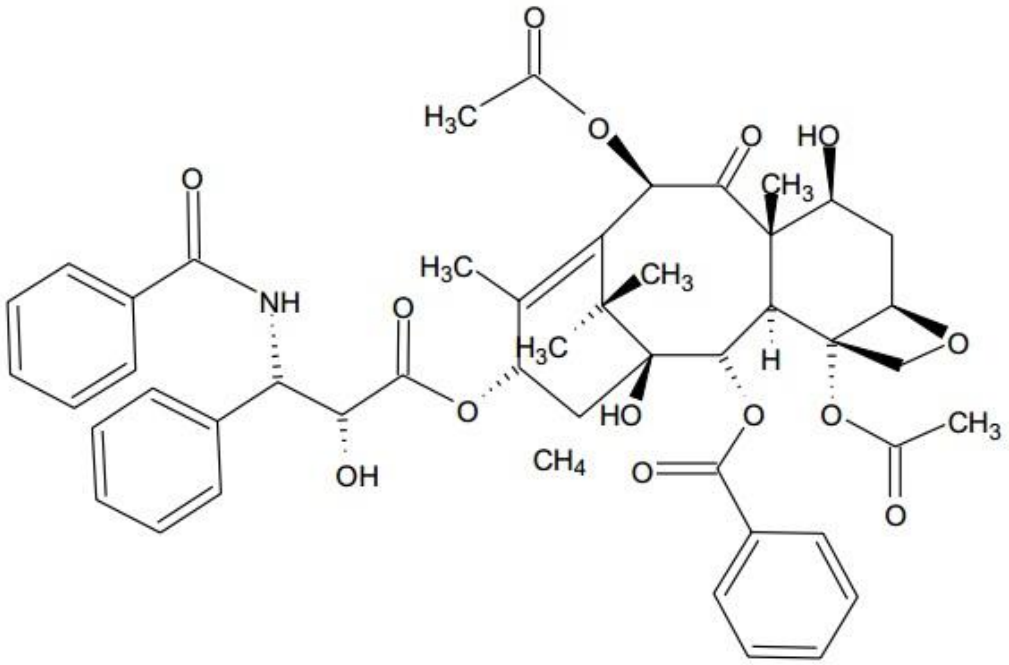

Fig. 2 *Chemical structure of paclitaxel. Adapted from (25).*

One of the most know characteristic of PTX is its high hydrophobicity. This comes as a disadvantage and classifies PTX under class IV of Biopharmaceutics Classification System due to its low solubility and poor permeability (26). To overcome this disability, the commercial form of PTX, Taxol®, uses Cremophor EL and dehydrated ethanol as a vehicle. After dilution in an isotonic solution, the drug is ready for an intravenous administration. However, there is a great number of side effects regarding this was of treatment such as hypersensitivity, hypotension, neurotoxicity or nephrotoxicity (27). Alternatives to Cremophor EL are under investigation, including Abraxane®, a Cremophor-free formulation using albumin-bound nanoparticles to transport paclitaxel that has been approved by the Food and Drug Administration (FDA) for breast cancer treatment (28). Genexol-PM is other example of a Cremophor-free formulation, this time using polymeric micelles (29).

2.1.3 Nanoparticles for drug delivery

Nanomedicine has been widely explored, implying the use of nanomaterials in clinical and research activities to diagnose and treat pathologies. Nanoparticles as drug delivery systems have been studied for more than 20 years and grown exponentially. From simple systems to multifunctional particles that might target specific cells, improving the properties of therapeutic carriers by increasing the circulation time, half-life, bioavailability, solubility and lower toxicity (5).

A way to improve the diagnosis and treatment of colorectal cancer is the use of nanoparticles as drug delivery system. These nanocarriers with small and tuneable size have a large surface area capable of being functionalized with all sorts of molecules, such as, proteins or DNA. They have suitable stability, high carrier capacity, including hydrophobic and hydrophilic drugs and are compatible with different routes of administration. By protecting the drug they carry, nanoparticles might increase drug circulation time, improving the effect with smaller concentrations (30). Some examples of clinically approved nanoparticles for cancer treatment are Doxil® (31) and Abraxane® (32), but more than 250 pharmaceutical nanocarriers in preclinical or clinical stage of development (33).

There are several types of nanoparticles. Liposomes (34), polymeric (35), magnetic (36), dendrimers (37) and nucleic acid based nanoparticles (38) have been widely be used in drug delivery. Polymeric nanoparticles are one of the most used and the focus of this work. This type of particle tends to be spherical, with a hydrophilic shell and a hydrophobic core, formed by self-assembly of two or more polymer blocks with different hydrophobic through aqueous or microencapsulation methods. These polymers are biodegradable and noncytotoxic, like poly (D, L-lactide-co-glycolide), polycaprolactone and chitosan. Polymeric nanoparticles are more stable

than liposomes, allowing the encapsulation of different types of chemical nature drugs and controlled in face of temperature or pH changes (33). This controlled release combined with the ability of encapsulate highly toxic, poorly soluble or unstable drugs make polymeric nanoparticles a promising nanocarrier (39).

Poly(lactic-co-glycolic-acid) (PLGA) is one of the polymers most used to produce nanoparticles (40). This copolymer of polylactic acid (PLA) and polyglycolic acid (PGA) is biocompatible and biodegradable and approved by US FDA and EMA (European Medicines Agency), making it suitable to use in drug delivery (41). To increase the circulation time of the particles and to avoid its immunogenicity, poly(ethylene glycol) (PEG) is often introduced in a drug delivery system (42). PEG is capable of shield particles from the immune system, especially from macrophages but is also capable to protect proteins from digestion by proteolytic enzymes and diminish clearance rates through renal filtration, increasing the serum half-life of partides (43). Combining PLGA and PEG is a common practice, including for paclitaxel delivery (28, 44-46)

The physical and chemical properties, such as size, shape or surface charge are important when a nanoparticle-based strategy is being planned. For cancer treatment, nanoparticles of around 200 nm are considered ideal since nanoparticles can permeate the tumour vasculature but no the normal vasculature (6). Solid tumour have imperfect vessels, with fenestrations around 100-600 nm, whereas a normal vessel have 1-2nm fenestrations (47, 48). This huge difference combined with an improper lymphatic drainage origin the effect known as Enhanced Permeability and Retention (EPR) effect. This effect allows the accumulation of nanopartides in the tumour site, improving its action (6, 19, 49).

This EPR effect can be the solo responsible for the success of a drug-loaded nanopartide in the cancer treatment but certainly is not the only alternative. Targeted nanoparticles have been an important focus of interest. These particles are capable increasing the *in vivo* specificity of a cancer therapy when are functionalized with a moiety capable of recognise specific cancer receptors (7). Several moieties can be used for this purpose, such as monoclonal antibodies (50), peptides (51) or aptamers (52).

Within these moieties, monoclonal antibodies (mAb) are widely used since they are capable of recognizing specific antigens in the surface of cells (53). Different receptors can be used for this purpose, one example is the Carcinoembryonic antigen (CEA).

2.1.4 Carcinoembryonic antigen

Carcinoembryonic antigen (CEA) is a highly glycosylated cell surface protein of 180 kDa. It was firstly described by Gold and Freeman, who detected this glycoprotein in human colon cancer tissue extracts (54). Involved in cell adhesion, this glycoprotein is also expressed in many other tumours, even though its normal expression period is during fetal development. It is known that healthy adult tissues express CEA, but only on the luminal surface of the cell and this

expression in minimal. In colorectal cancer, the expression pattern is much higher and is always aberrant, being expressed on the basal and lateral cell membranes (55). That way, making CEA accessible though the blood flow (56-58).

Thanks to the characterization of CEA-related proteins sequences and cloning of cDNA, the cloning of CEA-related family lead to the identification of the large family called carcinoembryonic antigen cell adhesion molecules (CEACAMs) (59-61). These proteins that in humans are encoded by 22 separate genes, 12 specific for CEACAMs (**Figure 3)** and 10 for pregnancy-specific glycoproteins (PSG). The extracellular domains of these molecules are necessary for the role as homophilic and heterophilic intercellular adhesion molecules. But CEA is also capable of associate with signaling receptors and influence signaling pathways to encourage metastasis progression (62-64).

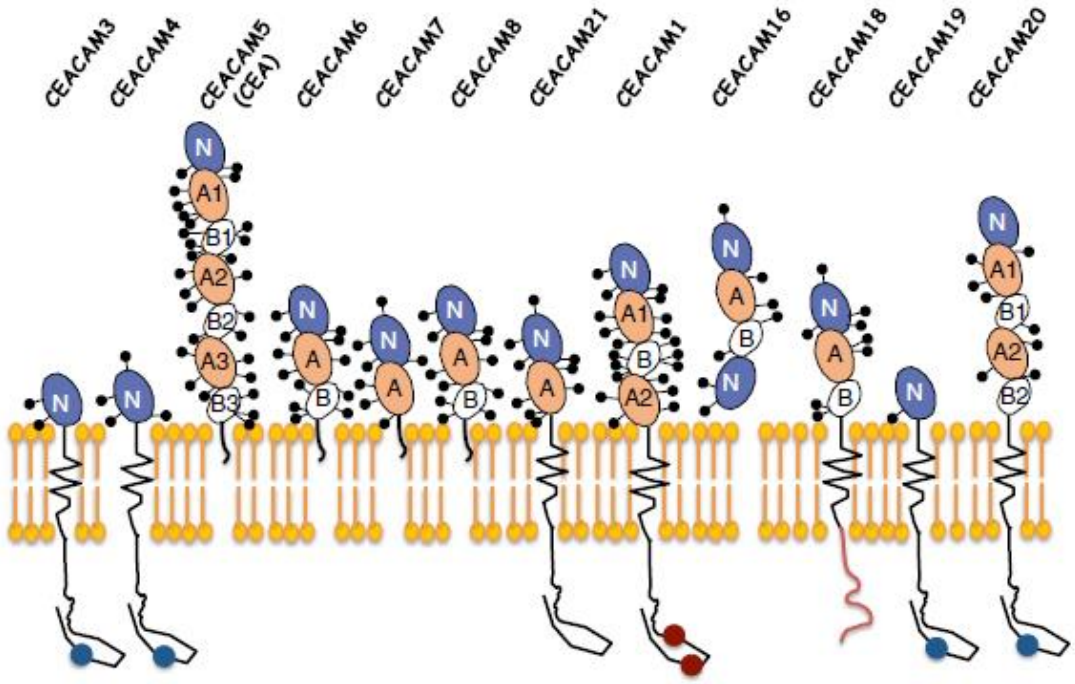

Fig. 3 *Carcinoembryonic antigen cell adhesion molecules (CEACAMs) family. Adapted from (65).*

Being a cell surface glycoprotein, CEA is a functional colon carcinoma ligand, critical to the metastatic dissemination of colonic carcinoma (57). This molecule is one of the most used tumour markers. The reason behind this is the fact that CEA is a stable molecule with restricted expression in normal tissues and highly expressed in tumours. In healthy individual, the majority of CEA is produced in colon, where it is released from the apical surface of cells, being expelled from the organism through feces. This means that its presence in the blood is neglected. In cancer situations, especially colorectal cancer, CEA is expressed around the cell since the last loosed its polarity (55). For example, CEACAM1 is one of the most distributed molecules, within CEA family. Of its 12 different isoforms (**Figure 4**), 3 are secreted. CEA can then be measured

in the serum of patients with colorectal or other carcinomas like pancreas, liver, breast, ovary or lung cancer. It is recommended by the "National Institute of Clinical Excellence European Group on Tumour Markers" and the "American Society of Clinical Oncology" and can be measured before and after surgery, as well as during chemotherapy. Better survival chances are associated with the intensive follow-up using CEA measurements since the rise and doubling time of CEA are sensitive in signalling recurrent disease (66, 67).

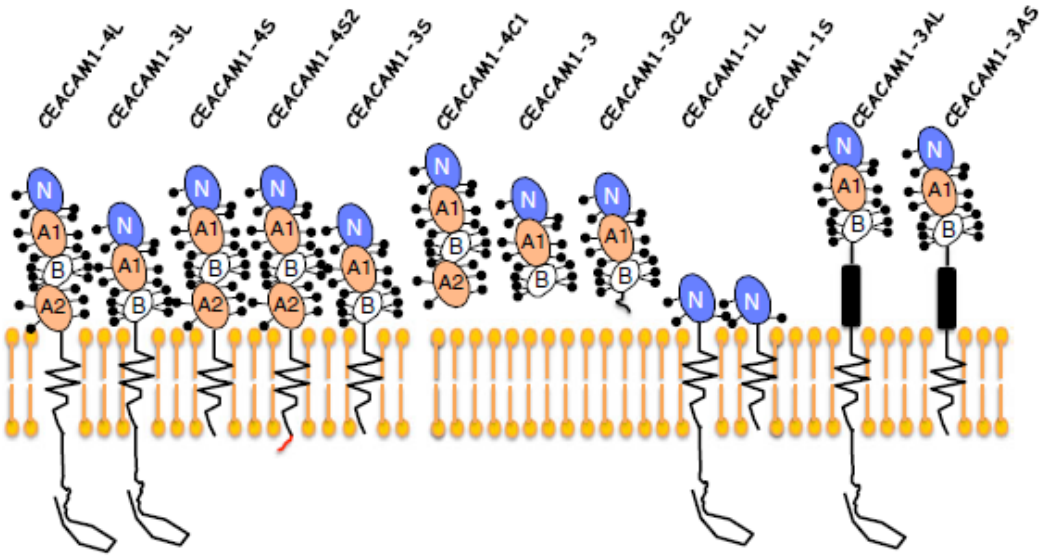

Fig. 4 *CEACAM1 different isoforms. Adapted from (65).*

Since it is expressed in primary and metastatic colorectal as well as other carcinomas, CEA is one of the most explored target for an antibody-mediated strategy (55, 57). Tiernan *et. all* tested four different molecules that act as biomarkers and CEA was proven to be the most suitable for tumour targeting for both diagnosis and therapeutic delivery purposes (53). Several antibodies or antibody fragments have been studied for diagnosis purposes. Radiolabled anti-CEA antibodies or antibody fragments have been used in mouse models using PET imaging for tumour visualization and the results were clear and promising. Even though most of the studies using specific CEA targeted antibodies conjugated with fluorophores were more of a "proof-of-concept", results showed improvement in highlighting the tumour, improving the surgical resection (68, 69). One example of an anti-CEA antibody is CEA-Scan™, a radiolabelled antibody approved in 1999 by the FDA for cancer imaging. It is implemented for patients with histologically-demonstrated colon or rectal carcinoma and as a technique for imaging of recurrence or metastatic carcinomas.(70, 71) Not only single antibodies are used been studied for diagnosis, but also functionalized nanoparticles are been studied to allow a better tumour visualization (72-79). Even though the most focus is on nanoparticles for diagnosis purposes, CEA is also explore as a moiety for drug delivery. Lipid-polymer NP is one example of this strategy (80).

Chapter 3

Materials and methods

3.1 Materials

Colorectal cancer cell lines, C2BBe1 Clone of Caco-2 (passage 66 to 80) was purchased from American Type Culture Collection (ATCC, USA) and SW480 (passage 12 to 35) was kindly provided by the University of Göttingen. Cervix adenocarcinoma cell line HeLa (passage 43 to 51) was also purchased from American Type Culture Collection (ATCC). Invasive breast ductal carcinoma cell line MCF-7 (passage 10 to 17) was kindly provided by Dr. Inês Alencastre (Institute of Investigation and Innovation in Health – i3S). PLGA (Purasorb® PDLG 5004A; 50:50) was kindly provided by Corbion and PLGA-PEG-COOH from PolySciTech®. Paclitaxel (PTX) was kindly provided by Indena SpA – Milano. 3-(4,5,-dimethylthiazol-2-yl)-2,5-diphenyltetrazolium bromide (MTT), Tween®80, 2-(N-morpholino)ethanesulfonic acid (MES), 1-ethyl-3-(3-dimethylaminopropyl)carbodiimide (EDC), N-hydroxysuccinimide (NHS), paraformaldehyde, sodium chloride, 6-coumaric (6-C), bovine serum albumin (BSA), phosphate-buffered saline (PBS), polyvinyl alcohol (PVA) and Pluronic F-127 were acquired from Sigma-Aldrich. Dimethyl sulfoxide (DMSO) and sulphuric acid were purchased from VWR. Centrifugal filters (Ultra-15, 100 kDa) were purchased from Amicon® Versene dialysis membrane (10,000 MWCO; Snake Skin® pleated dialysis tubing), CEA Monoclonal Antibody (COL-1) and TMB Substrate Solution, acetone and methanol were purchased from ThermoFisher. Anti-Cacino Embryonic Antigen antibody (CEA31) was acquired from Abcam, Triton X-100 from SpiChem and sodium azide from Panreac AppliChem. Goat anti-mouse- HRP antibody was purchased from EDM Millipore. Lastly, Dulbecco's modified Eagle medium (DMEM) was purchased from Lonza, fetal bovine serum, non-essential aminoacids (NEAA), penicillin and streptomycin were purchased from Merck Millipore.

3.2 Methods

3.2.1 Production of the nanoparticles

The nanoparticles were produced though a nanoprecipitation method. Briefly, 50mg of PLGA plus 2.5mg PLGA-PEG-COOH (w/w) were added to 10mg of PTX and left in 2mL of a mixture of DMSO and acetone (1:1) to allow the dissolution. This organic solution was transferred through a 25G needle to an aqueous solution of 1% Pluronic F-127 (20mL) under magnetic stirring (200 rpm). Final solution was left for 3h to allow the organic solvent evaporation. The washing process of the nanoparticles was performed using Amicon® filters (100kDa), centrifuged for 20 min at 1912x*g*. This process was repeated twice and the first supernatant was collected for PTX quantitation. After the last centrifugation, the nanoparticles were redispersed at the desired concentration. PTX-loaded PLGA nanoparticles were produced in a similar manner, only without adding PLGA-PEG-COOH. The empty nanoparticles also used the same procedure, without adding the drug. 6-coumarin loaded nanoparticles were produced following the same method but instead of PTX, 0.1% (w/w) of coumarin dissolved in DMSO was added.

3.2.2 Physical and chemical characterization

3.2.2.1 Mean particle size, size distribution and surface charge

After washing, all the formulations of nanoparticles were tested for its average size and polydispersity index with Dynamic Light Scattering (DLS) and surface charge was assessed through Electrophoretic Light Scattering (ELS), using a Malvern Zetasizer Nano ZS. The samples were diluted in sodium chloride (NaCl) 10Mm, pH 7.4.

3.2.2.2 Morphology

The morphology of the nanoparticles was observed though Transmission Electron Microscopy (TEM), after washing. Briefly, 10 µL of PTX-loaded PLGA-PEG nanoparticles were mounted on nickel grids and a beryllium holder and left to stain for two minutes. The excess liquid was removed with filter paper. Afterwards a Uranyl Acetate solution was added and left

to incubate for 2 seconds. The JEOL JEM 1400 TEM was used at 120kV and the images were digitally recorded using a CCD digital camera Orious 1100 W.

3.2.2.3 Association Efficiency and Drug Loading

The Association Efficiency (AE) and Drug Loading (DL) of PTX into nanoparticles were assessed by High Performance Liquid Chromatography (HPLC, Merck-Hitachi 7000), by the indirect method. This method uses the supernatant of the nanoparticle after washing and quantifies the drug that was not associated to the particle. A calibration curve of PTX dissolved in methanol was produced, using concentrations from 1 to 100 µg/mL. The supernatants of different formulations were collected and tested through a LiChrospher® 100 RP-18 (5µm) (Merck Millipore) with guard column. The mobile phase was composed of methanol and water (65:35) at a flow rate of 1.0 mL/min. The injection volume was 20 µL and the absorbance wavelength was 227nm. The values of AE and DL were calculated using the following Equation **2.1** and **2.2** (81).

$$Association\ Efficacy\ (\%) = \frac{initial\ mass\ of\ PTX - recovered\ mass\ of\ PTX}{initial\ mass\ of\ PTX} \times 100 \quad \textbf{(2.1)}$$

$$Drug\ Loading\ (\%) = \frac{initial\ mass\ of\ PTX - recovered\ mass\ of\ PTX}{theoretical\ mass\ of\ nanoparticle} \times 100 \quad \textbf{(2.2)}$$

3.2.3 *In vitro* paclitaxel release studies

The *in vitro* release profile of PTX from PLGA and PLGA-PEG nanoparticles was performed sing a dialysis membrane, were 1mL of the nanoparticle (1mg/mL of PTX) or free drug solution (1 mg/mL) was placed and the membrane was immerged in 40 mL of PBS (pH 7.4, 0.1% Tween 80®). The samples were stirred at 100 rpm at 37ºC, 0.5mL of each sample was removed in the predetermined time points (0.25, 0.5, 0.75, 1, 2, 4, 8, 24 and 48h) and the same volume was refilled with fresh medium. The concentration of PTX was determined by HPLC analysis, as described above.

The addition of Tween®80 to the release medium (PBS) was performed to aid the solubility of PTX and to prevent it to bind to the dialysis membrane. Since PTX is highly hydrophobic, an optimal concentration of Tween®80 had to be assessed. A previously experiment was performed using six different concentrations of Tween®80 (0, 0.5, 1, 2, 5 and 10%) in PBS. Five milligrams

of PTX were added to the release medium and samples were taken at three time points (15 min, 1h and 24h). The conditions where the samples were kept were the same as in the release study. A second release study was performed using 10% Tween 80 instead of 0.1% in order to assess if a higher concentration of Tween 80 could improve the release. The same protocol as performed using 0.1% Tween was followed.

3.2.4 6-coumarin loaded nanoparticles

To obtain fluorescent NPs, a similar protocol to the nanoparticle production was followed, being 6-coumarin (6-C) (0.1% w/w loading) encapsulated instead PTX. The particles were characterized with the same techniques as previously mentioned for PTX-loaded NP. The *in* vitro release profile was also accessed and the 6-C was quantified by fluorescence spectroscopy (exc. 460 nm, emi. 510 nm). To ensure the sink conditions, to the release medium, PBS 1x, was added 0.1% Tween® 80 to allow the solubility of 6-C. The nanoparticles (1 mL; with a concentration of 1 mg/1 mL) were placed in a dialysis membrane and this membrane immersed in 40 mL of the release medium, at 37°C with constant stirring (100 rpm). At specific time points (0.25; 0.5; 0.75; 1, 2, 4, 8 and 24h), a 500 µL sample was taken and the same amount was replaced with fresh release medium. The samples were put in a 96-well plate reader and their fluorescence quantified.

3.2.5 Cell Culturing

The cell culture medium used for all cell lines was Dulbecco's modified Eagle medium (DMEM) supplemented with 10% (v/v) fetal bovine serum (FBS), 1% (v/v) of non-essential aminoacids (NEAA) and 1% (v/v) of penicillin (100 Ul/ml) and streptomycin (100 Ul/ml). Cells were maintained at 37°C, 5% CO_2 and 95% humidity, and media was renewed every 2-3 days.

3.2.6 Specificity of the anti-CEA antibodies to cell lines

Before the functionalization of the nanoparticles and cell-nanoparticle interaction studies, an antibody validation experiment was performed to access the specificity of the antibodies to the cell lines used. Two different antibodies were used, COL-1 and CEA31 against four cell lines Caco-2 clone, MCF-7, HeLa and SW480. To do so, $2x10^5$ cells per well resuspended in FACs buffer (PBS plus 10% FBS and 0.1% of sodium azide) were seeded in a 96 well plate with round bottom.

The plate was centrifuged for 3min in 300 x *g* and the supernatant removed. The cells were incubated with the primary antibody (COL-1 or CEA31) during 1h in order to allow the antibody binding to the surface of the cells. The 1h time point was also used in the other cell-assays. Then the cells were washed three times before adding the anti-mouse secondary antibody. After leaving 1h to incubate, the cells were washed three times more and analysed in the FACS CANTO II cytometer (BD Biosciences).

3.2.7 Surface-functionalization of the nanoparticles

In order to functionalize the surface of nanoparticles with anti-CEA antibody, the carbodiimide chemistry was selected to chemically link the antibody ligand (82, 83). Nanoparticles (1mL) were centrifuged at 6000 rpm for 20 min and then resuspended in 500 µL of MES buffer (0.1M). Then, 43 µg of EDC and 64 µg of NHS were dissolved in 500 µL of the MES buffer and added to the nanoparticle dispersion. The mixture was left in agitation for 1h, at room temperature. Three washes in MiliQ water (centrifuged at 6850x*g*, for 20 min) proceeded to remove the excess of EDC and NHS, where the nanoparticles, and the last resuspension was performed with PBS 1x, pH 7.4. The antibody, COL-1, was then introduced in a ratio of 1:0.01 (COOH:Ab) and left for 24h in agitation at 4°C. Before storing the functionalized particles, two washes were performed using PBS 1x, in order to remove the excess of antibody.

3.2.8 Binding efficiency of the antibody

3.2.8.1 Nuclear magnetic resonance

Proton Nuclear magnetic resonance (^{1}H NMR) was used to confirm the presence of antibody in the surface of nanoparticles. Functionalized and non-functionalized PLGA-PEG nanopartides (1 mL) were lyophilised and then dissolved in 600 µL DMSO, as well as 1.9 µg of the antibody alone. The samples were placed on the nuclear magnetic resonance quartz tubes and analysed. The analysis was performed on an Advance III HD spectrometer from Bruker operating at 600 MHz (14.1 Tesla), at room temperature and chemical shift values were expressed in δ (ppm). The internal reference was tetramethylsilane (TMS).

3.2.8.2 Enzyme-linked immunosorbent assay

The binding efficiency of CEA antibody to nanoparticles was further confirmed by and enzyme-linked immunosorbent assay (ELISA). The protocol consisted in plating 10 µL of each sample (input (same amount of antibody used in the functionalization process), nanopartide (functionalized and non-functionalizes) and the supernatant of both types of nanoparticles) added to 40 µL of carbonate coating buffer and left to incubate at 37°C for 3h. Three washes with PBST were done and a solution of BSA 1% was added to each sample to prevent non-specific binging of the antibodies to the plate. The plate was left to incubate at 37°C for 1h. Afterwards, three more washes were performed and 50 µL of Goat anti-mouse- HRP antibody (1:2500) were added and left to incubate for 45 min at 37°C. After washing for the last 3 times, TMB Substrate Solution was added to each sample and left during 20 min. Then sulphuric acid 2M was added and the plate read at abs=450 nm. The conjugation efficiency (%) was calculated using the following equation:

$$Conjugation\ efficiency = \frac{absorvance\ of\ the\ sample}{absorvance\ of\ the\ input} \times 100 \quad \textbf{(2.3)}$$

The input, as described, is the same amount of antibody used in the functionalization process. It acts as a positive control for this experiment.

3.2.9 Cytotoxicity assessment of the nanoparticles

To test the cytotoxicity of the nanoparticles, a MTT assay was performed against intestinal epithelial cells. Caco-2 clone (C2BBe1) and SW480 cell lines were the chosen cell lines, the first as a CEA-positive cell line and the second the sub-expressing. The cells were cultured in different culture flasks in a complete medium. $1x10^4$ cells per well were seeded in a 96-well plate and left to incubate for 24h at 37ºC in a 5% CO_2 air atmosphere. After removing the medium, the cells were washed twice with PBS. Five different concentrations of free drug, empty PLGA nanoparticles, empty PLGA-PEG nanoparticles, loaded PLGA nanoparticles and PLGA-PEG nanoparticles (0.01, 0.1, 1, 10 and 100 nM) were prepared with complete medium and left to incubate with the cells for 24h. The cells were washed twice with PBS and incubated with the MTT solution (final concentration 0.5 mg/ml) for 4h, at 37ºC in the dark. The MTT solution was then removed and DMSO was added and left to incubate for 15 min under stirring, at room temperature. The absorbance was measured at 570 nm and 630 nm using a microplate spectrophotometer. The following equation was used to analyse the results:

$$Metabolic\ activity\ (\%) = \frac{experimental\ value - negative\ control}{positive\ control - negative\ control} \times 100 \quad \textbf{(2.4)}$$

The negative control used was Triton X-100 1% and the positive control was medium with only live cells (84).

3.10 Cell-nanoparticle interaction studies

In order to find the optimal concentration of particles to use in the cell-nanoparticle interaction studies, $1x10^5$ cells (Caco-2 or SW480) per well were seeded in a 24-well plate and left to incubate for 24h. After two washes with PBS 1x, a solution of 6-C loaded PLGA PEG nanoparticles in culture medium (5, 50 or 500 µg/mL) was added to the cells and left to incubate for 15 min or 1 hour. After two washes, the cells were detached with versene and centrifuged at 500 x *g* for 5min. After the resuspension in FACS buffer, the cells were analysed in FACS CANTO II.

The same protocol described above was followed to test the interaction of functionalized and non-functionalized nanoparticles with Caco-2 clone and SW480 cell lines. The concentration of particles used in the assay was 50 µg/mL.

3.11 Data analysis

Every experiment was performed in triplicate and is represented as mean ± standard deviations (SD). A one-way analysis of variance (ANOVA) with Tukey's post hoc test (GraphPadPrism software Inc., USA) was used to analyse the data. The level of significance was set at probabilities of $*p < 0.05$; $**p < 0.01$ and $***p < 0.001$.

Chapter 4

Results and Discussion

PTX-loaded PLGA nanoparticles and PTX-loaded PLGA-PEG nanoparticles were produced by nanoprecipitation and the critical physical chemical properties, such as mean size, size distribution, surface charge, association efficiency and drug loading were accessed. The surface of the particles was functionalized using the carbodiimide chemistry and its efficiency was tested though ELISA. The cytotoxicity of the particles, functionalized and non-functionalized, was evaluated though a cell metabolic assay (MTT). Flow cytometry studies were performed in order to characterize the interaction between functionalized and non- functionalized nanoparticles and two intestinal epithelial cell lines. The results are presented and discussed in this chapter.

4.1 Synthesis and characterization of PLGA nanoparticles

4.1.1 Particle size, size distribution and zeta potential

The first attempt in this project was the establishment of parameters to attain the optimal nanoparticle formulation. As it can be seen in **Table 1**, several formulations were prepared in the optimization process. Formulations were being produced and evaluated on size, polydispersity index and surface charge in order to achieve an ideal formulation. These formulations were expected to result in size below 200 nm, to be able to permeate through the tumour vasculature but not through the normal vasculature (6). The polydispersity value had to be as below 0.1, to ensure a highly monodisperse population and a surface charge of ± 30mV, since that is considered the zeta potential of electrostatically stabilized nanosuspensions (85). However, lower values of surface charge have been associated with stability, especially with PEGylates nanoparticle (86, 87). Guided by these values, the mass of PLGA and drug used were the first variables to be changed. The high amount of PLGA (100 and 60 mg) were not well dissolved in the organic solvent, even when the volume of the solvent was double. Considering that and since the size of particles with less polymer (10 and 20 mg) did not presented significantly differences in size from the formulation using 50 mg, the last was the amount chosen. The presence of PEG on the surface was important for this formulation since prolongs the circulation time of nanoparticles in the blood system by escaping easily the uptake by macrophages (42). To determine the best ratio for the final formulation, 1%, 2% and 5% of PLGA-

PEG-COOH ratios were tested. There were no significant differences between these three formulations in size, so the higher amount, 5% (2.5 mg), was chosen in order to increase the pegylation advantages for the system.

The amount of drug used was chosen accordingly to the association efficacy and drug loading. When the amount of polymer and drug were defined, the surface charge was taken in consideration, and the values were too close to zero. This was not expected since the PLGA used has a negative group, COOH, and the charge should be more negative. One of the hypothesis for these results was the surfactant, PVA that could be attached to the surface and did not detached during the washing procedure. Pluronic F-127 was then chosen since the surface charge of the particles using this surfactant was more negative. The charge of the particles in this work is important not only to avoid nanoparticle aggregation but also for the functionalization process since the chosen chemistry was the carbodiimide (88). This chemistry is one of the most used to conjugate nanoparticles and antibodies with reactive functional groups such as amino-NH_2 (e.g. lysine) (89). To allow this covalent bound, the nanoparticle must have COOH groups on its surface, and its present detected trough a negative surface charge. The values were not as negative as expected (83), but the use of sodium chloride used in the characterization process can influence the values, making them more neutral (90).

The final formulation used 50 mg of PLGA, 2.5 mg of PLGA-PEG-COOH and 10 mg of paclitaxel, dissolved in 2 mL of organic solution (acetone and DMSO 1:1) and Pluronic F-127 as the surfactant.

Table 1 *Properties of all formulations produced during the optimization process, including the mean size, polydispersity index, surface charge association efficacy and drug loading. The values are represented as mean values ± SD (n=3).*

Surfactant (%)	PLGA (mg)	PLGA-PEG0-COOH (mg)	Paclitaxel (mg)	Organic solution (mL)	Size (nm)	PdI	Surface charge (mv)	Association efficacy (%)	Drug loading (%)
PVA 2%	100	0	0	1	318 ± 17	0.27 ± 0.05	-3.1 ± 0.3	-	-
			10		301 ± 13	0.23 ± 0.03	-3.4 ± 0.2	-	-
			0	2	273 ± 19	0.11 ± 0.02	-2.2 ± 0.5	-	-
			10		267 ± 4	0.12 ± 0.03	-2.7 ± 0.6	-	-
	60	0	0	1	436 ± 29	0.22 ± 0.05	-2.0 ± 0.6	-	-
			6		272 ± 19	0.18 ± 0.03	-1.4 ± 0.1	68.2 ± 0.9	6.6 ± 0.1
	50	0	0	2	229 ± 2	0.06 ± 0.03	-3.8 ± 0.9	-	-
			10		232 ± 5	0.11 ± 0.07	-2.3 ± 0.3	95.7 ± 2.5	19.0 ± 0.5
		0.5	0	2	226 ± 3	0.08 ± 0.04	-3.2 ± 1.1	-	-
			10		233 ± 5	0.10 ± 0.03	-2.2 ± 0.4	97 ± 0.3	19.3 ± 0.1
		1	0	2	221 ± 3	0.06 ± 0.02	-2.4 ± 0.7	-	-
			10		231 ± 4	0.09 ± 0.03	-2.1 ± 0.5	94.8 ± 3.1	18.9 ± 0.6
		2.5	0	2	218 ± 4	0.05 ± 0.03	-2.7 ± 0.4	-	-
		2.5	10	2	235 ± 7	0.09 ± 0.03	-1.9 ± 0.4	97.0 ± 0.6	19.3 ± 0.1
	20	0	0	1	228 ± 5	0.04 ± 0.03	-1.7 ± 0.2	-	-
			2		234 ± 6	0.09 ± 0.03	-1.4 ± 0.3	91.7 ± 9.5	9.1 ± 1.0
			1		227 ± 3	0.09 ± 0.04	1.7 ± 0.7	45.1 ± 18.3	8.2 ± 3.6
	10	0	2	1	213 ± 16	0.18 ± 0.06	5.6 ± 1.9	67.3 ± 13.4	3.3 ± 0.7
Pluronic F-127 1%	50	0	0	2	184 ± 9	0.18 ± 0.03	-11.8 ± 2.1	-	-
			10		197 ± 10	0.2 ± 0.04	-9.4 ± 3.7	99 ± 0.8	19.8 ± 0.2
		2.5	0	2	173 ± 2	0.07 ± 0.02	-10.0 ± 0.7	-	-
			10		177 ± 4	0.14 ± 0.03	-5.7 ± 2.1	99.2 ± 0.1	19.8 ± 0.04

4.1.2 Morphology

The final formulation of nanoparticles was analysed thought TEM. **Figure 5** shows the morphology of PTX-loaded PLGA-PEG nanoparticles and it can be seen that the nanopartides were spherical in shape and with a similar size, below 200 nm. The size is according to the DLS results, even though in the image, the size seam smaller. The shape is another feature important since spherical particles tend to be more easily internalized (91). It can be seen that the partides have a spherical shape, as intended.

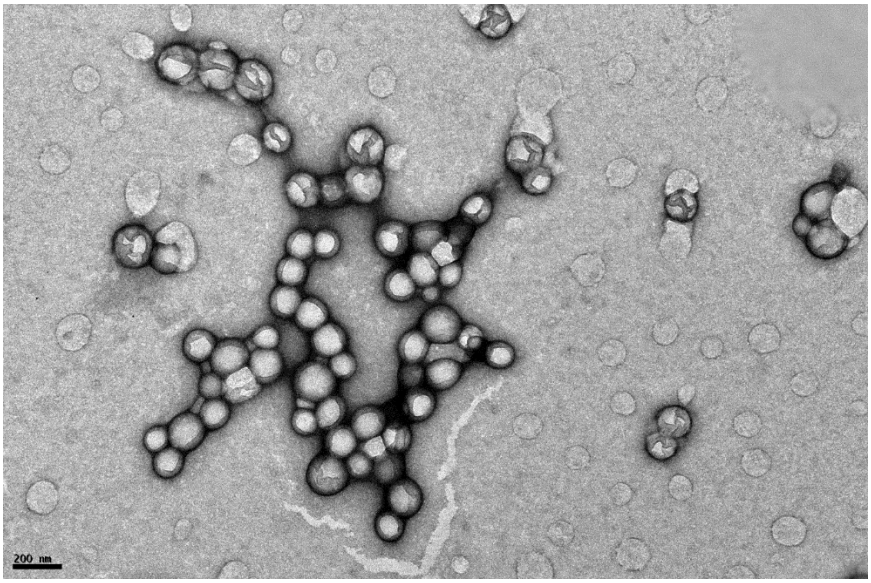

Fig. 5 *Image of PTX-loaded PLGA PEG nanoparticles obtained by Transmission Electron Microscopy (TEM).*

4.1.3 Association Efficiency and Drug Loading of Paclitaxel

The Association Efficiency (AE) and Drug Loading (DL) of the PTX-loaded nanoparticles was assessed, using the different formulations, by HPLC. The average retention time of PTX was around 12 minutes.

The supernatant of the different formulations was analysed and the amount chosen of paclitaxel was decided through the results. The formulation with 10 mg of PTX presented the higher AE and DL, 99.2% and 19.8%, respectively (**Table 1**), becoming the chosen amount of drug. Due to the high hydrophobicity of PTX, high values of association efficiency were expected when using the nanoprecipitation technique. This was observed in previous published work using PTX-loaded nanoparticles (92).

4.2 *In vitro* paclitaxel release

Paclitaxel is a highly hydrophobic drug with a solubility in PBS of only 0.3 µg/mL (93). Tween®80 is often used to help solubilizing PTX, usually at 0.1% which increases its solubilisation to 6.32 µg/mL (46, 94-96). The *in vitro* studies of free PTX, PTX-loaded PLGA and PLGA-PEG nanoparticles were then performed and the cumulate profile is shown in **Figure 6**.

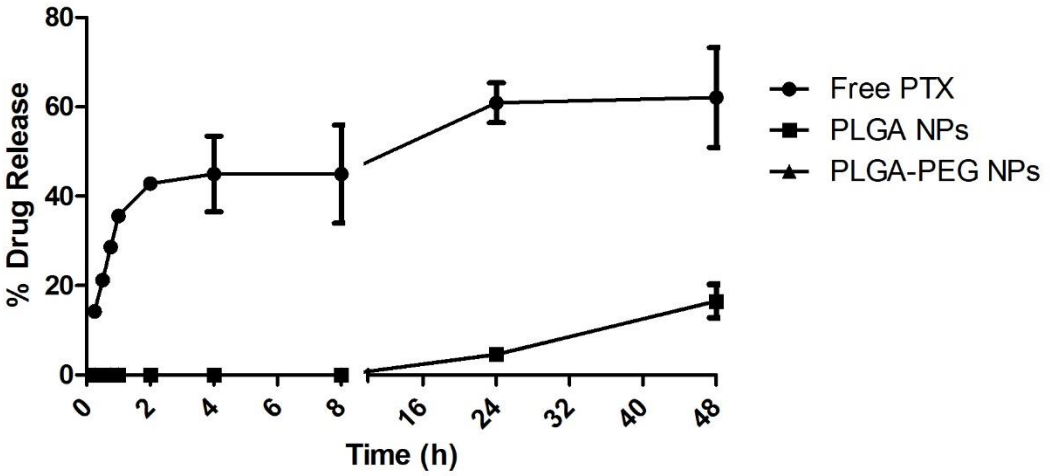

Fig. 6 *Cumulative percentage release of free PTX (circles), PLGA nanoparticles (squares) and PLGA-PEG nanoparticles (triangles) in 0.1% Tween. The percentage of drug release was accessed for 48 hours. Values represented as a mean ± SD (n=3).*

The release of free PTX only reached around 60% during the 48h. In PLGA-PEG nanopartides the release of PTX was only observed after 8h and reached a maximum of 17% in 48h. In previous experiments, free PTX controls reached 100% (97). Also, other types of nanoparticles were used and the release started earlier than 24h (46, 95). This could mean that the nanopartides produced in this work are more stable and allows a more controlled drug release.

To assess if the absence of signal from drug release in the nanoparticle formulations until the 8h was because the drug was not being release from the particle or because the drug did not solubilise well in the release medium, other experiment was performed.

It is described that the solubility of paclitaxel in PBS increases with the addition of Tween®80 in a concentration-dependent manner (46). To determine the ideal Tween® 80 concentration, a previous experiment was performed with different concentrations of Tween®80 (0.5, 1, 2, 5 and 10%) where 5 mg of paclitaxel were introduced and left at 37°C, under continuous stirring (100 rpm) for 24h. At specific time points, a sample was collected to be tested though HPLC. The results showed higher solubility for the 10% Tween®80, being this percentage the choose one to use in the release study of the nanoparticles. The *in vitro* release profile of the free PTX, PLGA and PLGA-PEG-COOH nanoparticles was then assessed using 10% Tween®80 in PBS (pH7.4). The cumulative release profile is shown in **Figure 7**.

For the PLGA-PEG nanoparticles, it can be observed that the first burst of drug release happens during the first hour, around 30% (**Figure 7 B**). From that time point until the 8h time point, the release happens in a slower rhythm, until around 40%. After that time point and until the 48h time point, the release seems to stop. The PLGA nanoparticle s and the free PTX show a similar release profile, even though the last shows a slight increase, but not statistically significant.

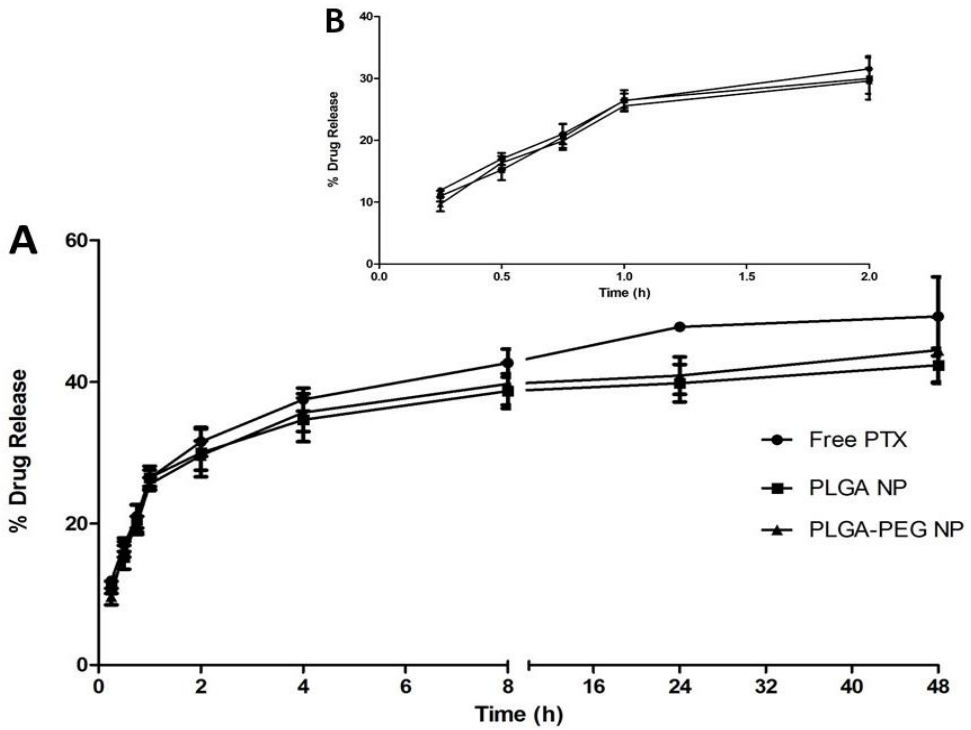

Fig. 7 *Cumulative percentage release of free PTX (circles), PLGA nanoparticles (squares) and PLGA-PEG nanoparticles (triangles). The % of drug release was accessed for 48 hours (A) and presented the burst of release during the first 2h (B). Values represented as a mean ± SD (n=3).*

These results could mean that using 10% Tween®80, PTX is released from the nanopartides in an earlier stage, because the drug in more soluble in the release medium. However, it is more probable that the results between free PTX and PTX-loaded particles were so similar because Tween®80 is destroying the particles, releasing the drug. This hypothesis is supported with previous publish work that used this concentration of Tween®80 to produce nanoparticles (98).

Thus, results from the first release study (**Figure 6**) are more reliable and state that these PLGA and PLGA PEG nanoparticles are a robust vehicle for PTX, only allowing its release after 24h.

4.3 6-Coumarin loaded nanoparticles

To produce fluorescent PLGA-PEG nanoparticles, 6-coumarin (6-C) was encapsulated during the production process. The mean particle size, PdI and surface charge was tested and the results were 201 nm, 0.07 and -13 mV, respectively. Comparing with particles encapsulating PTX, the size increased around 30 nm, but still considered similar, making the fluorescent particles capable of mimic the PTX-loaded particles in the cell assays.

The *in vitro* release of 6-C loaded nanoparticles was also assessed in a similar matter, using 0.1% Tween®80 in PBS (pH 7.4) as a release medium. The experiment was conducted at 37°C and under constant stirring (100 rpm). 6-C was detected through fluorescence (exc. 460 nm, emi. 510 nm). A calibration curve was performed with concentrations from 0.002 to 0.008 µg/mL, with R^2 value of 0.99. The results, found in the **Figure 8**, show a controlled release until 24h of only 8%, which is not considerable significate. More important, less than 1% of 6-C was released up to 1h. Considering that most assays that used these particles had a maximum incubation time of 1h, the fluorescence observed in the cell assays presented below is duo to the presence of fluorescent particles and not because of free 6-C.

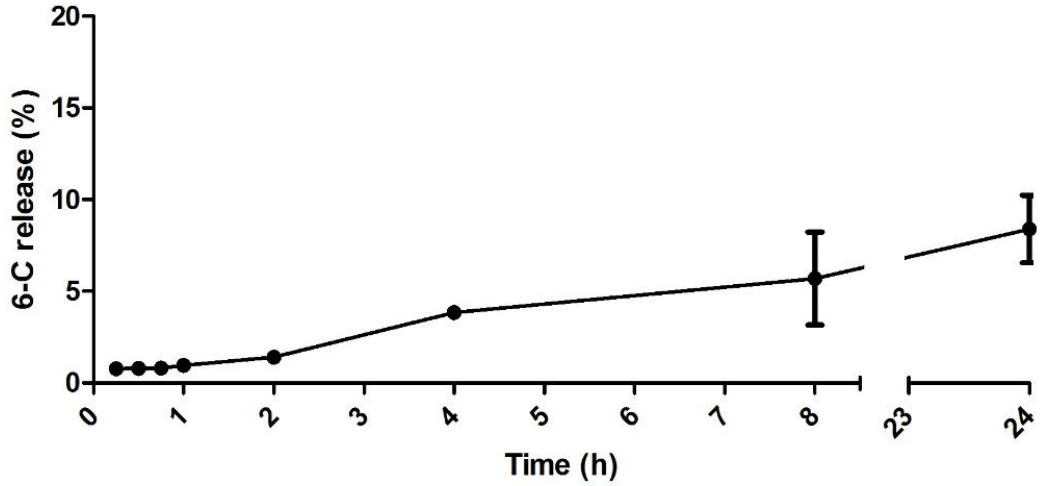

Fig. 8 *Cumulative release profile of 6-C from PLGA-PEG nanoparticles. At the presented time points, an aliquot was taken from the release medium and fresh medium was introduced. The amount of 6-C release was quantified by fluorescence (ex. 410nm, em. 510nm). Values represented are mean values ± SD (n=3).*

4.4 Specificity of the antibodies and cell lines

The cell lines chosen to perform the cell assays were Caco-2 clone and SW480. The reason behind this choice lies on the expression of CEA and because these cell lines are form intestinal adenocarcinomas. SW480 had been described as a low-expressive CEA cell line and Caco-2 as a positive cell line for CEA expression (56). Since the cell line chosen was Caco-2 clone and not Caco-2, and SW480 has been described by some as a CEA-expressing cell line, a pre-study was necessary to determine the CEA expression on the surface of the cells.

Two antibodies anti-CEA were used, CEA31 and COL-1. These antibodies had not been tested against Caco-2 clone and SW480 before, so a known positive and negative cell line was necessary. In this case, MCF-7 was used as a described positive cell line and HeLa as a negative cell line.

The assay performed to confirm this expression was Flow Cytometry. The four cell lines were incubated with the two antibodies, a fluorescent secondary antibody afterwards and then the samples analysed. As can be seen in **Figure 9**, HeLa and SW80 had similar levels of fluorescence which can validate SW480 as a negative cell line for the expression of CEA. The only significant difference between the two cell lines was with the CEA31 antibody (*P<0.05), which HeLa presented higher fluorescent units (FU) than SW480. MCF-7 and Caco-2 clone had higher levels of fluorescence, which can indicate them as positive cell lines for the CEA expression. It is important to note that Caco-2 clone had values significantly higher than MCF-7, especially with the COL-1 antibody (***P<0.001). This antibody showed better interaction with almost all cell lines, except in the HeLa cell line.

Accordingly with the results, SW480 was chosen as the negative cell line and Caco-2 clone as the positive cell line for all cell assays. The antibody chosen to functionalize the particles was COL-1 because of its higher interaction levels with the cell lines chosen.

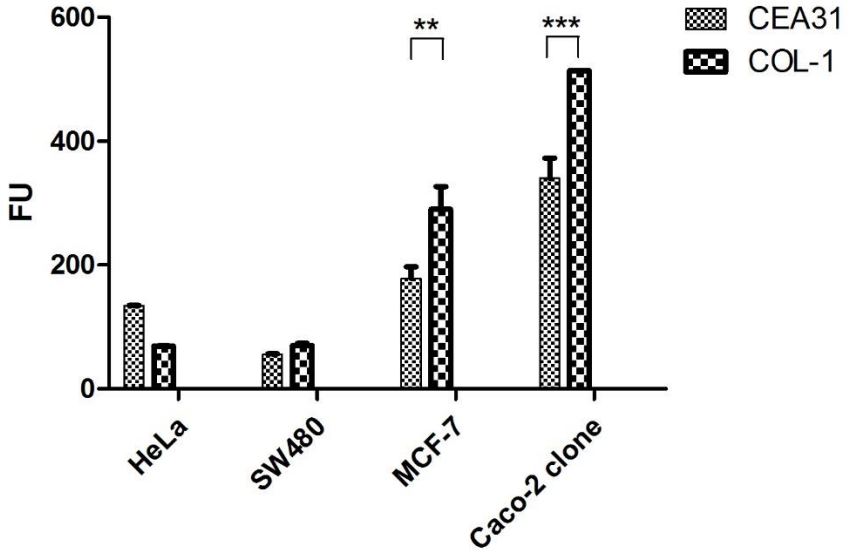

Fig. 9 *Fluorescent units (FU) values for the interaction between CEA31 antibody and COL-1 antibody with HeLa, SW480, MCF-7 and Caco-2 clone line lines. The results are mean values ± SD (n=3; **P<0.01; ***P<0.001).*

4.5 Binding efficiency of the antibody

The next step was the functionalization of the surface with the model antibody against CEA, COL-1. Using a carbodiimide chemistry, the COOH groups of the nanoparticles were activated through ECD/NHS. EDC reacts with the carboxylated NPs when NHS is present in the reaction, forming amine-reactive groups. When incubated with the antibody COL-1, its primary amines are coupled to the COOH groups of the nanoparticles through a stable amide bound (99). The ratio used in this functionalization was 1:0.01 (COOH:Ab). The mean size, PdI and surface charge of functionalized and non-functionalized PTX-loaded PLGA-PEG nanoparticles was accessed. Both types of particles went through the functionalization process, the difference was the non-addition of antibody on the non-functionalized particles. The results (**Table 2**) showed a slight increase in size for the functionalizes particles but not a decrease in the surface charge, as expected since the negative groups (COOH) should be used in the conjugation process (83). Comparing the results of non-functionalizes PLGA-PEG particles in **Table 1** with **Table 2**, a size incensement can be observed. This is explained by the functionalization process, due to the presence of EDC/NHS linked to the surface of NPs or due to aggregation since nanopartide aggregation was already described when using cabodiimide process (100).

Table 2 *Properties of functionalized and non-functionalized PTX-loaded PLGA-PEG nanoparticle, including the mean size, polydispersity index and surface charge. The values are represented as mean values ± SD (n=3).*

	Size (nm)	PdI	Surface charge (mv)
Functionalized PTX-loaded PLGA-PEG NP	243 ± 10	0.3 ± 0.04	-10.4 ± 2.3
PTX-loaded PLGA-PEG NP	213 ± 12	0.2 ± 0.05	-6.5 ± 0.3

4.5.1 Nuclear Magnetic Resonance

One of the methods used to confirm the presence of COL-1 antibody in the nanoparticle formulation was Proton Nuclear Magnetic Resonance (^{1}H NMR). Free antibody, functionalized and non-functionalized PLGA-PEG nanoparticles were dissolved in DMSO. The three spectra were compared in order to assess if the characteristic peak of the antibody was present in the functionalized nanoparticles but not in the non-functionalized nanoparticles. The results shown in **Figure 10** show similar peaks in all samples from the solvent (DMSO) at 2.5 ppm and from TMS at 0.0 ppm. Both non-functionalized and functionalized nanoparticles had common peaks at 1.5, 5.0 and 5.5 ppm, characteristic of PLGA (101). A peak should also be visible at around 3.5 ppm detecting the presence of PEG. In the spectra obtained, there was, indeed, a large peak around 3.5 ppm for both functionalized and non-functionalized nanoparticles. However, it was also present in the free antibody spectra as well, which was not expected. It can also be seen that a specific peak common in the antibody and functionalized particles was not seen. Antibodies usually have spectra with much more peaks compared to the peaks seen in **Figure 10**, which might indicate that this technique was not sensible enough to detect the antibody, or the amount of antibody used (1.9 µg) was too low (102).

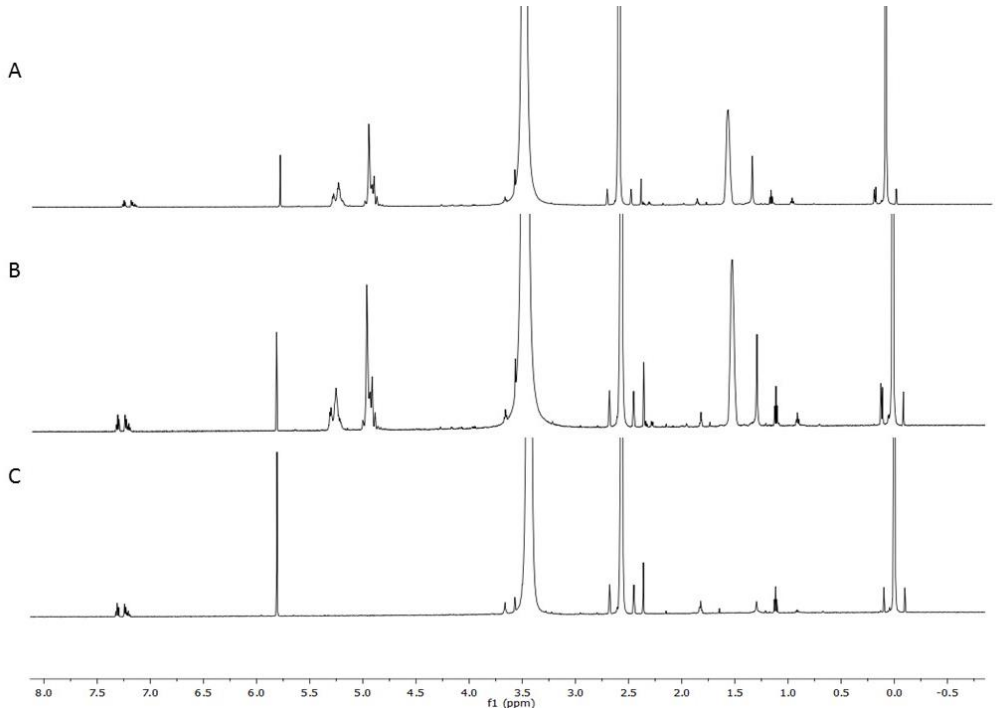

Fig. 10 *H^1 NMR spectra of non-functionalized (A) and functionalized (B) PLGA-PEG nanoparticles and the free antibody (C).*

Thus, the NMR results are not able to conclude the presence of the antibody. A more sensible method should be used to assess the efficacy of the functionalization process.

4.5.2 Enzyme-linked immunosorbent assay

Another method to confirm the functionalization was an Enzyme-linked immunosorbent assay (ELISA). An input of the same amount of antibody used in the functionalization was used as a positive control. The non-functionalized nanoparticles and supernatants were used as negative controls. The nanoparticles functionalized and the supernatant of the first wash after functionalization was then tested to confirm the functionalization. The results, shown in **Figure 11**, confirm the present of antibody in the nanoparticle surface. Around 15% of antibody is present in the surface of the particle, even though the amount of antibody in the supernatant was higher, around 40%. The total amount of the input should be equal to the some between the nanoparticle and supernatant, but the input seams higher. This could mean that some of the antibody is lost, probably during the following washes. Even though 15% is a low percentage, the amount of antibody used was significantly lower than the mass of polymer (100-fold less). A higher amount of antibody could lead to a higher association efficacy but even with excessive amounts of antibody, low conjugation efficacy, 1-20%, has been reported when using carbodiimide chemistry (99). Another possibility that can lead to this low percentage is the orientation of the antibody. If the antibody do not have the binding site available for the

secondary antibody-HRP, the signal is not strong, even though the antibody is in fact in the surface of the particle (103). A more efficient conjugation method was not applied in this work since the antibody did not have a specific group, just as a cysteine group, that would allow the use of maleimide chemistry (82).

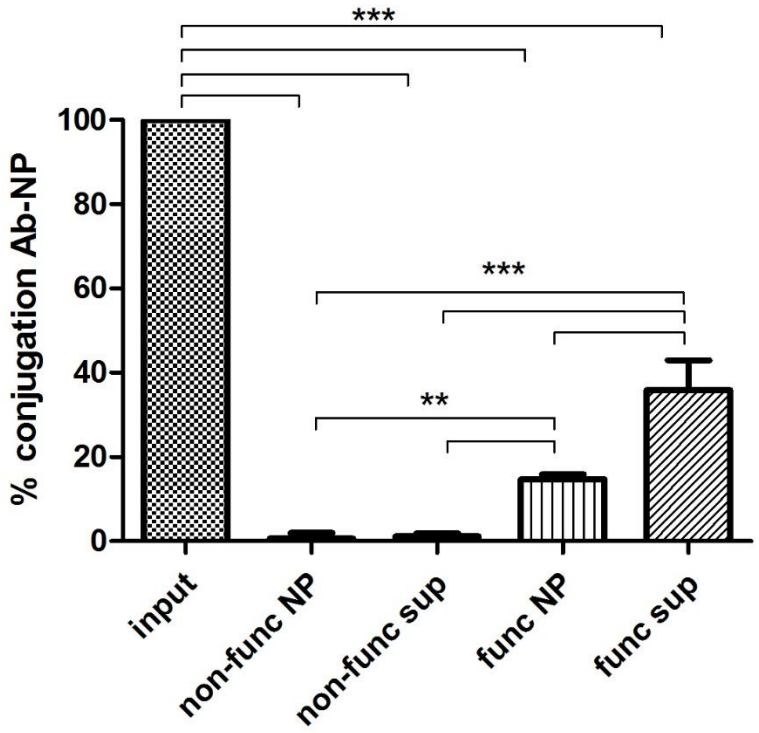

Fig. 11 *Percentage conjugation between the antibody and the nanoparticle surface. The initial amount of antibody used in the functionalization (input), nanoparticles and supernatants of functionalized and non-functionalized nanoparticles were tested using an ELISA assay to assess the presence of the antibody, confirming the functionalization. The presented values as means ± SD (n=3; **P<0.01; ***P<0.001).*

4.6 Cytotoxicity assessment of the nanoparticles

The cytotoxicity of the nanoparticles was tested using the MTT assay, a colorimetric assay used to assess the cell metabolic activity (104). Free PTX, functionalized and non-functionalized empty PLGA or PLGA-PEG and loaded PLGA or PLGA-PEG nanoparticles were tested, each in five different concentrations (0.01, 0.1, 1, 10 and 100nM). These concentrations were chosen accordingly to the half minimal inhibitory concentration (IC50) of PTX that is in the range from 2.5 to 7.5 nM (105). Two intestinal epithelial cell lines were used, Caco-2 clone and SW480, to perform this *in vitro* assay, with the incubation period with the samples of 24h.

As seen in **Figure 12**, most formulations have values above 70%, which according to International Organization for Standardization, means that no significant toxicity was identified

(81). The results were expected since the release of PTX from the nanoparticles is not completed after only 24h. Some exception are depicted, such as in non-functionalized empty PLGA-PEG NP (100 nM) (**Figure 12 A**) or non-functionalized PTX-loaded PLGA NP (10 nM or 100 nM) (**Figure 12 B**), where the metabolic activity was close to 50%. Despite appearing slightly different from the other nanoparticle formulations, differences were not significant. It was expected that metabolic activity would decrease with the increase of PTX concentration, as can be seen in all experiments.

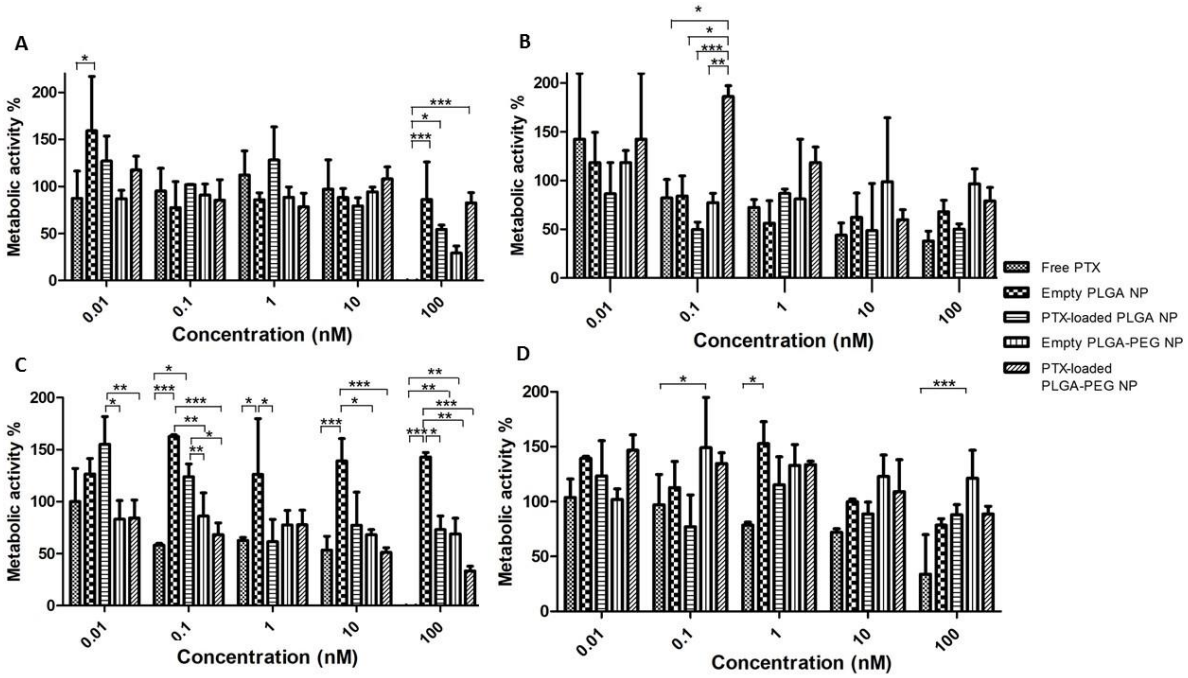

Fig. 12 *Metabolic activity SW480 cell line (A, C) and Caco-2 clone cell line (B, D) with free PTX, empty and loaded PLGA or PLGA-PEG non-functionalized (A, B) and functionalized (C, D) nanoparticles at concentrations of PTX (0.01, 0.1, 1, 10 and 100nM) after incubation for 24h. Cell viability was determined by MTT assay. Untreated cells were taken as positive control and 1% Triton X-100 was used as negative control. Values are reported as mean ± SD (n=3; *P<0.05; **P<0.01; ***P<0.001).*

Four different types of nanoparticle were tested, not only assess the safety of the formulations but also to identify differences between them. The present of PEG in the formulation did not decrease this value and empty particles provided higher values of activity when compared with PTX-loaded nanoparticles, which was expected. Between functionalized and non-functionalized nanoparticles there was no significant differences, except in empty PLGA NP (0.01 nM) and PTX-loaded PLGA PEG NP (10 and 100 nM) in SW480 cell line (**Figure 12 A and C**). Since these differences were not noticeable in Caco-2 cell line, the antibody may not be considered the responsible for an increase in toxicity.

The most important conclusion is that this nanoparticle system is safer to the cells that the free drug, proving the efficacy of the system since the drug load can be high (100 nM) without damaging the cells, decreasing the secondary effects.

4.7 Cell-Nanoparticle interaction studies

4.7.1 Optimization of particle concentration for cell-nanoparticle interaction studies

After proving the functionalization of the nanoparticles by ELISA, the next study to be performed was the cell-nanoparticle interaction study. To be able to determine the right number of nanoparticles used in the assay, a pre-study was performed using bare particles with three different concentrations (5, 50 and 500 µg/mL). This study is important to determine a base line data for the unspecific interaction between the nanoparticles and the cells, as well as the background fluorescence of the cells itself. The particles were left to incubate with Caco-2 clone and SW480 cell lines for 15min and 1h.

The results presented in **Figure 13** are blank corrected, as cells without nanoparticles being the blank. The lowest concentration presented negative values because of the blank correction, proving to be unfit to use as the signal is as low as the background. The 50 µg/mL concentration, although not much different from the 5 µg/mL, presented values slightly above background (**P<0.01 for Caco-2 clone). The maximum concentration had a significantly increased signal (***P<0.001) which could interfere with the final purpose of distinguish a difference between functionalized and non-functionalized nanoparticles. In can also be seen in Figure 7 that SW480 cell line present significantly lower values of FU when compared to Caco-2 clone cell line. The chosen concentration to procced with the *in vitro* interaction studies was 50 µg/mL.

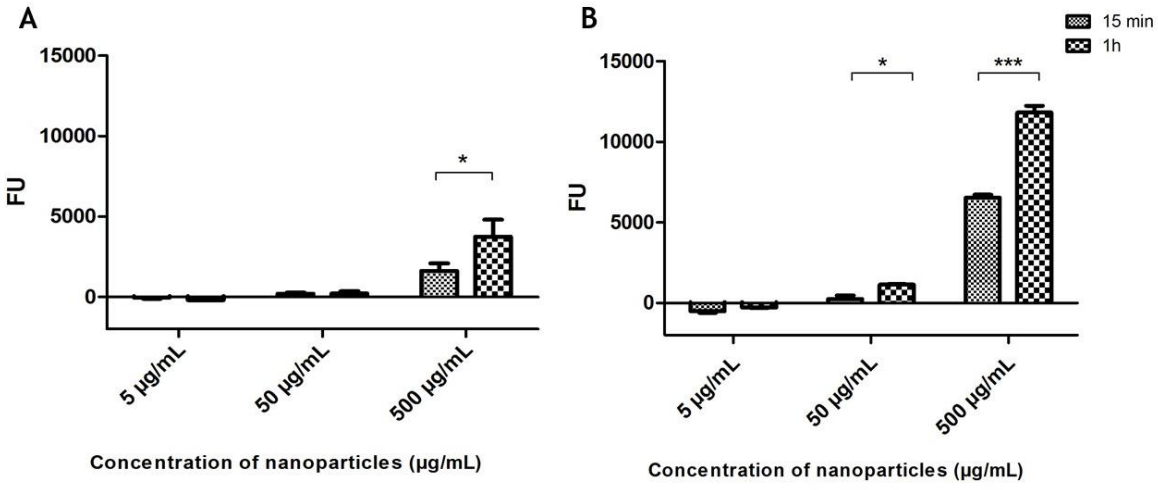

Fig. 13 *Fluorescent units of unspecific interaction between SW480 (A) or Caco-2 clone (B) cell line and PLGA-PEG nanoparticles, with concentrations of 5, 50 and 500 µg/mL, for 15 min and 1h. The represented values are mean values ± SD and blank corrected (n=3; *P<0.05; ***P<0.001).*

4.7.2 Cell-nanoparticle interaction study

The functionalized nanoparticles were then tested by FACS, as described above. Non-functionalized and functionalized particles, with a concentration of 50 µg/mL were dispersed in cell culture medium and incubated with cells for 15 minutes and 1 hour. Normally the nanoparticles are dispersed in PBS or culture medium without supplements, but since the purpose of the nanoparticles was to be administered by the intravenous route, the protein corona expected to be form upon administration can be mimicked with complete medium, also full of proteins (106).

The results presented in **Figure 14** showed higher fluorescent values for the Caco-2 clone cell line in all samples, as expected since it is the positive cell line, compared to SW480 cell line. The between the different time points, there is an increase in the fluorescent values in the 1 hour time point for both cell lines and type of particles. Statistic differences were observed between the two different time points, ($P<0.001$) for both functionalized and non-functionalized NP in SW480 cell line (**Figure 14 A**) and ($P<0.01$) for non-functionalized NP and ($P<0.001$) for functionalized NP in Caco-2 cell line (**Figure 14 B**). Between the functionalized and non-functionalized nanoparticles there is not any significant difference, even though a trend can be observed with slight higher values for the functionalized particles. This result can be a side effect of the chosen conjugation chemistry. Even though carbodiimide chemistry is one of the most used, when applied in this case, it is not site-specific. Antibody possesses several NH_2 groups, and so, when the COOH groups of the nanoparticles are activated, any NH_2 of the antibody can be attached. The challenge comes with the direction of the antibody. If the antigen biding zone of the antibody is not available, the particle will not correctly bind to the receptor. A site-oriented chemistry, such as maleimide-thiol, could improve the binding efficacy of the system by using a modified antibody, or other moiety such as a peptide, with a thiol group in the Fc region. That way, the antigen binding region would be available to bind to the receptor (88, 107).

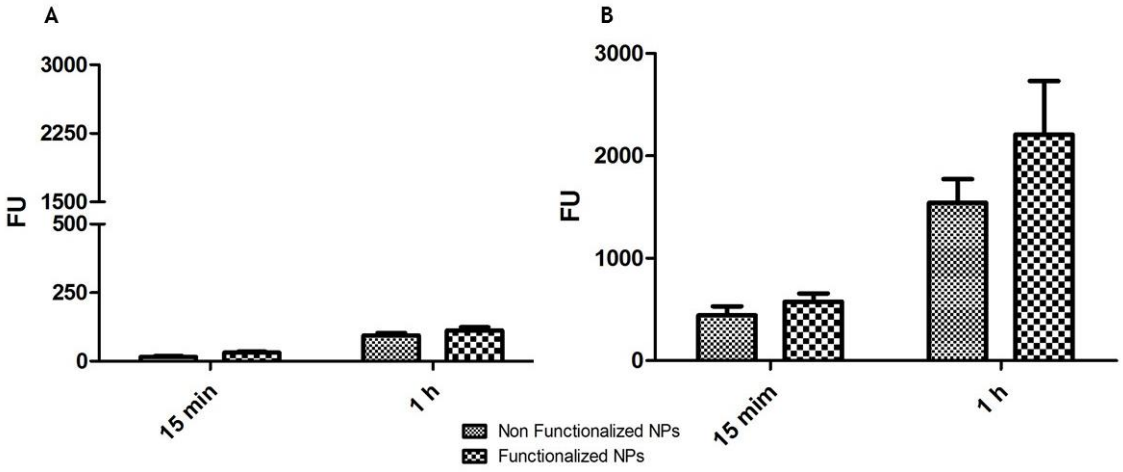

Fig. 14 *Fluorescent units of cell-NP interaction studies in SW480 (A) and Caco-2 clone (B) cell line. Values represented as mean values ± SD (n=3)*

Chapter 5

Conclusion

In this work, PLGA-PEG nanoparticles were produced by nanoprecipitation. The most important physical-chemical properties were assessed, namely mean size, polydispersity index and surface charge. The results showed particles of around 177 nm, with a PdI of 0.14 and a zeta-potential of -6mV. Mean particle size around 200 nm are considered appropriate for drug delivery in cancer treatment, which is the ultimate goal of these particles. The PdI value, even though above 0.1, is still considerable a monodisperse population. For an intravenous injection, a monodisperse and negatively charged population is important to ensure that the nanopartides are not going to aggregate when injected. PTX was loaded to these particles as an anticancer drug model. The association efficiency and drug loaded were tested by HPLC and the results were 99% and 20%, respectively. The morphology of the nanoparticles was accessed through Transmission Electron Microscopy and the particles presented a round shape and uniform sizes, agreeing with DLS results. The *in vitro* release study showed a controlled release, proving the robustness of the system. Cytotoxicity studies were performed to ensure the safety of the particles, where empty or PTX-loaded nanoparticles were tested on two intestinal cell lines, Caco-2 clone and SW480. Particles were proven safe since the viability of the cells was mainly above 70%.

The functionalization of PLGA PEG nanoparticles with antibodies on the surface allow nanoparticles to become able of target specific tissues. In this case, an antibody against CEA was used in order to target colorectal cancer cells. Carbodiimide chemistry, one of the most used, was the chosen method to perform the functionalization process and ELISA assay was used to verify the efficacy of functionalization. The results demonstrated a successful process even though some improvement could be done.

The next step was the cell and nanoparticle interaction studies. By using fluorescent nanoparticles and COL-1 as anti-CAE antibody, functionalized nanoparticles were then tested against the positive, Caco-2 clone, and negative, SW480 cell lines. The results showed higher interaction with the positive cell line, as expected, although no significantly differences between functionalized and non-functionalized particles were observed. Even though, functionalized particles tented to present higher values of interaction.

In conclusion, the nanoparticles proved to be a suitable vehicle for drug delivery purposes, non-toxic and capable of interact with colorectal carcinoma cell lines.

Future Work

Even though the system built is robust, there is always room for improvement. The functionalization process is one example. The carbodiimide chemistry is this case was not site-oriented, but other method of functionalization or modification in the antibody can be used to ensure the antibody binds to the surface of the nanoparticle in its correct direction, leaving antigen binding zone of the antibody available to interact with CEA from cancer cells.

Other moieties can be explored to the functionalization, like small peptides or antibody fragments that with equal binding affinity, make the particle less prone to immune reactions after the injection of the particles through intravenous route.

Fluorescent microscopy studies can be done to evaluate the qualitative interaction of the nanoparticles with cells, allowing a better knowledge about the internalization process of the particles. Some permeability studies through the intestinal tissue can be performed as well. Following the intention of administration these nanoparticles by intravenous route, a 3D model can be established with endothelial cells on top and epithelial cells on the bottom, simulating the intestinal epithelial. After proving interaction with intestine cancer epithelial cells, the nanoparticles would be ready to move to *in vivo* studies. These studies would evaluate the biodistribution, safety and therapeutic effect of the system.

References

1. Siegel RL, Miller KD, Fedewa SA, Ahnen DJ, Meester RG, Barzi A, et al. Colorectal cancer statistics, 2017. CA: a cancer journal for clinicians. 2017;67(3):177-93.
2. Favoriti P, Carbone G, Greco M, Pirozzi F, Pirozzi R, Corcione F. Worldwide burden of colorectal cancer: a review. Updates in surgery. 2016;68(1):7-11.
3. Anitha A, Maya S, Sivaram AJ, Mony U, Jayakumar R. Combinatorial nanomedicines for colon cancer therapy. Wiley Interdisciplinary Reviews: Nanomedicine and Nanobiotechnology. 2016;8(1):151-9.
4. Couvreur P. Nanoparticles in drug delivery: Past, present and future. Advanced Drug Delivery Reviews. 2013;65(1):21-3.
5. Wang AZ, Gu F, Zhang L, Chan JM, Radovic-Moreno A, Shaikh MR, et al. Biofunctionalized targeted nanoparticles for therapeutic applications. Expert opinion on biological therapy. 2008;8(8):1063-70.
6. Torchilin VP. Targeted pharmaceutical nanocarriers for cancer therapy and imaging. The AAPS journal. 2007;9(2):E128-E47.
7. Cisterna BA, Kamaly N, Choi WI, Tavakkoli A, Farokhzad OC, Vilos C. Targeted nanoparticles for colorectal cancer. Nanomedicine. 2016;11(18):2443-56.
8. Tiernan J, Perry S, Verghese E, West N, Yeluri S, Jayne D, et al. Carcinoembryonic antigen is the preferred biomarker for in vivo colorectal cancer targeting. British journal of cancer. 2013;108(3):662-7.
9. Mishra J, Drummond J, Quazi SH, Karanki SS, Shaw J, Chen B, et al. Prospective of colon cancer treatments and scope for combinatorial approach to enhanced cancer cell apoptosis. Critical reviews in oncology/hematology. 2013;86(3):232-50.
10. Saúde D-Gd. Portugal - Doenças Oncológicas em Números - 2015 2016 [Available from: https://www.dgs.pt/em-destaque/portugal-doencas-oncologicas-em-numeros-201511.aspx.
11. Huxley RR, Ansary-Moghaddam A, Clifton P, Czernichow S, Parr CL, Woodward M. The impact of dietary and lifestyle risk factors on risk of colorectal cancer: a quantitative overview of the epidemiological evidence. International journal of cancer. 2009;125(1):171-80.
12. Saif MW, Chu E. Biology of colorectal cancer. The Cancer Journal. 2010;16(3):196-201.
13. Bartoş A, Bartoş D, Szabo B, Breazu C, Opincariu I, Mironiuc A, et al. Recent achievements in colorectal cancer diagnostic and therapy by the use of nanoparticles. Drug metabolism reviews. 2016;48(1):27-46.
14. Nakaji S, Umeda T, Shimoyama T, Sugawara K, Tamura K, Fukuda S, et al. Environmental factors affect colon carcinoma and rectal carcinoma in men and women differently. International journal of colorectal disease. 2003;18(6):481-6.
15. Miller KD, Siegel RL, Lin CC, Mariotto AB, Kramer JL, Rowland JH, et al. Cancer treatment and survivorship statistics, 2016. CA: a cancer journal for clinicians. 2016;66(4):271-89.
16. Kristjansson SR, Nesbakken A, Jordhøy MS, Skovlund E, Audisio RA, Johannessen H-O, et al. Comprehensive geriatric assessment can predict complications in elderly patients after elective surgery for colorectal cancer: A prospective observational cohort study. Critical Reviews in Oncology/Hematology. 2010;76(3):208-17.
17. Marshall JL. Managing potentially resectable metastatic colon cancer. Gastrointestinal cancer research: GCR. 2008;2(4 Suppl 2):S23.
18. Chabner BA, Roberts Jr TG. Chemotherapy and the war on cancer. Nature reviews Cancer. 2005;5(1):65.

19. Fernandes E, Ferreira JA, Andreia P, Luís L, Barroso S, Sarmento B, et al. New trends in guided nanotherapies for digestive cancers: A systematic review. Journal of Controlled Release. 2015;209:288-307.
20. Field KM, Kosmider S, Jefford M, Jennens R, Green M, Gibbs P. Chemotherapy treatments for metastatic colorectal cancer: is evidence-based medicine in practice? Journal of oncology practice. 2008;4(6):271-6.
21. Hill BT, Moran E, Etiévant C, Perrin D, Masterson A, Larkin A, et al. Low-dose twice-daily fractionated X-irradiation of ovarian tumor cells in vitro generates drug-resistant cells overexpressing two multidrug resistance-associated proteins, P-glycoprotein and MRP1. Anti-cancer drugs. 2000;11(3):193-200.
22. Wani MC, Taylor HL, Wall ME, Coggon P, McPhail AT. Plant antitumor agents. VI. Isolation and structure of taxol, a novel antileukemic and antitumor agent from Taxus brevifolia. Journal of the American Chemical Society. 1971;93(9):2325-7.
23. Singla AK, Garg A, Aggarwal D. Paclitaxel and its formulations. International journal of pharmaceutics. 2002;235(1):179-92.
24. Le Broc-Ryckewaert D, Carpentier R, Lipka E, Daher S, Vaccher C, Betbeder D, et al. Development of innovative paclitaxel-loaded small PLGA nanoparticles: study of their antiproliferative activity and their molecular interactions on prostatic cancer cells. International journal of pharmaceutics. 2013;454(2):712-9.
25. Trynda-Lemiesz L. Paclitaxel–HSA interaction. Binding sites on HSA molecule. Bioorganic & Medicinal Chemistry. 2004;12(12):3269-75.
26. Kasim NA, Whitehouse M, Ramachandran C, Bermejo M, Lennernäs H, Hussain AS, et al. Molecular properties of WHO essential drugs and provisional biopharmaceutical classification. Molecular pharmaceutics. 2004;1(1):85-96.
27. Szebeni J, Alving CR, Muggia FM. Complement activation by Cremophor EL as a possible contributor to hypersensitivity to paclitaxel: an in vitro study. JNCI: Journal of the National Cancer Institute. 1998;90(4):300-6.
28. Danhier F, Lecouturier N, Vroman B, Jérôme C, Marchand-Brynaert J, Feron O, et al. Paclitaxel-loaded PEGylated PLGA-based nanoparticles: in vitro and in vivo evaluation. Journal of Controlled Release. 2009;133(1):11-7.
29. Lee KS, Chung HC, Im SA, Park YH, Kim CS, Kim S-B, et al. Multicenter phase II trial of Genexol-PM, a Cremophor-free, polymeric micelle formulation of paclitaxel, in patients with metastatic breast cancer. Breast cancer research and treatment. 2008;108(2):241-50.
30. Thakor AS, Gambhir SS. Nanooncology: the future of cancer diagnosis and therapy. CA: a cancer journal for clinicians. 2013;63(6):395-418.
31. Barenholz Y. Doxil® — The first FDA-approved nano-drug: Lessons learned. Journal of Controlled Release. 2012;160(2):117-34.
32. Green M, Manikhas G, Orlov S, Afanasyev B, Makhson A, Bhar P, et al. Abraxane®, a novel Cremophor®-free, albumin-bound particle form of paclitaxel for the treatment of advanced non-small-cell lung cancer. Annals of Oncology. 2006;17(8):1263-8.
33. Kamaly N, Xiao Z, Valencia PM, Radovic-Moreno AF, Farokhzad OC. Targeted polymeric therapeutic nanoparticles: design, development and clinical translation. Chemical Society Reviews. 2012;41(7):2971-3010.
34. Garg T, K Goyal A. Liposomes: targeted and controlled delivery system. Drug delivery letters. 2014;4(1):62-71.
35. Chan JM, Valencia PM, Zhang L, Langer R, Farokhzad OC. Polymeric nanoparticles for drug delivery. Cancer Nanotechnology: Methods and Protocols. 2010:163-75.
36. Arruebo M, Fernández-Pacheco R, Ibarra MR, Santamaría J. Magnetic nanoparticles for drug delivery. Nano Today. 2007;2(3):22-32.
37. Caminade A-M, Turrin C-O. Dendrimers for drug delivery. Journal of Materials Chemistry B. 2014;2(26):4055-66.

38. Zhao Y-X, Shaw A, Zeng X, Benson E, Nyström AM, Högberg Br. DNA origami delivery system for cancer therapy with tunable release properties. ACS nano. 2012;6(10):8684-91.
39. Farokhzad OC, Cheng J, Teply BA, Sherifi I, Jon S, Kantoff PW, et al. Targeted nanoparticle-aptamer bioconjugates for cancer chemotherapy in vivo. Proceedings of the National Academy of Sciences. 2006;103(16):6315-20.
40. Sharma S, Parmar A, Kori S, Sandhir R. PLGA-based nanoparticles: A new paradigm in biomedical applications. TrAC Trends in Analytical Chemistry. 2016;80:30-40.
41. Kumari A, Yadav SK, Yadav SC. Biodegradable polymeric nanoparticles based drug delivery systems. Colloids and Surfaces B: Biointerfaces. 2010;75(1):1-18.
42. Veronese FM, Pasut G. PEGylation, successful approach to drug delivery. Drug discovery today. 2005;10(21):1451-8.
43. Hermanson GT. Bioconjugate techniques: Academic press; 2013.
44. El-Hammadi MM, Delgado ÁV, Melguizo C, Prados JC, Arias JL. Folic acid-decorated and PEGylated PLGA nanoparticles for improving the antitumour activity of 5-fluorouracil. International journal of pharmaceutics. 2017;516(1):61-70.
45. Liang C, Yang Y, Ling Y, Huang Y, Li T, Li X. Improved therapeutic effect of folate-decorated PLGA–PEG nanoparticles for endometrial carcinoma. Bioorganic & medicinal chemistry. 2011;19(13):4057-66.
46. Yang T, Cui FD, Choi MK, Cho JW, Chung SJ, Shim CK, et al. Enhanced solubility and stability of PEGylated liposomal paclitaxel: in vitro and in vivo evaluation. International Journal of Pharmaceutics. 2007;338(1-2):317-26.
47. Yuan F, Leunig M, Huang SK, Berk DA, Papahadjopoulos D, Jain RK. Mirovascular permeability and interstitial penetration of sterically stabilized (stealth) liposomes in a human tumor xenograft. Cancer research. 1994;54(13):3352-6.
48. Yuan F, Dellian M, Fukumura D, Leunig M, Berk DA, Torchilin VP, et al. Vascular permeability in a human tumor xenograft: molecular size dependence and cutoff size. Cancer research. 1995;55(17):3752-6.
49. Iyer AK, Khaled G, Fang J, Maeda H. Exploiting the enhanced permeability and retention effect for tumor targeting. Drug discovery today. 2006;11(17):812-8.
50. Kennedy PJ, Oliveira C, Granja PL, Sarmento B. Antibodies and associates: Partners in targeted drug delivery. Pharmacology & Therapeutics. 2017;177(Supplement C):129-45.
51. Ruoslahti E. Tumor penetrating peptides for improved drug delivery. Advanced Drug Delivery Reviews. 2017;110(Supplement C):3-12.
52. Farokhzad OC, Jon S, Khademhosseini A, Tran T-NT, LaVan DA, Langer R. Nanopartide-aptamer bioconjugates. Cancer research. 2004;64(21):7668-72.
53. Carter T, Mulholland P, Chester K. Antibody-targeted nanoparticles for cancer treatment. Immunotherapy. 2016;8(8):941-58.
54. Benchimol S, Fuks A, Jothy S, Beauchemin N, Shirota K, Stanners CP. Carcinoembryonic antigen, a human tumor marker, functions as an intercellular adhesion molecule. Cell. 1989;57(2):327-34.
55. Hammarström S, editor The carcinoembryonic antigen (CEA) family: structures, suggested functions and expression in normal and malignant tissues. Seminars in cancer biology; 1999: Elsevier.
56. Fichera A, Michelassi F, Arenas RB. Selective expression of carcinoembryonic antigen promoter in cancer cell lines. Diseases of the colon & rectum. 1998;41(6):747-54.
57. Bhatti I, Patel M, Dennison AR, Thomas MW, Garcea G. Utility of postoperative CEA for surveillance of recurrence after resection of primary colorectal cancer. International Journal of Surgery. 2015;16:123-8.
58. Conaghan P, Ashraf S, Tytherleigh M, Wilding J, Tchilian E, Bicknell D, et al. Targeted killing of colorectal cancer cell lines by a humanised IgG1 monoclonal antibody that binds to membrane-bound carcinoembryonic antigen. British Journal of Cancer. 2008;98(7):1217-25.

59. Oikawa S, Nakazato H, Kosaki G. Primary structure of human carcinoembryonic antigen (CEA) deduced from cDNA sequence. Biochemical and biophysical research communications. 1987;142(2):511-8.
60. Shively JE, Beatty JD. CEA-related antigens: molecular biology and clinical significance. Critical reviews in oncology/hematology. 1985;2(4):355-99.
61. Beauchemin N, Benchimol S, Cournoyer D, Fuks A, Stanners C. Isolation and characterization of full-length functional cDNA clones for human carcinoembryonic antigen. Molecular and cellular biology. 1987;7(9):3221-30.
62. Öbrink B. CEA adhesion molecules: multifunctional proteins with signal-regulatory properties. Current opinion in cell biology. 1997;9(5):616-26.
63. Samara RN, Laguinge LM, Jessup JM. Carcinoembryonic antigen inhibits anoikis in colorectal carcinoma cells by interfering with TRAIL-R2 (DR5) signaling. Cancer research. 2007;67(10):4774-82.
64. Li Y, Cao H, Jiao Z, Pakala SB, Sirigiri DNR, Li W, et al. Carcinoembryonic antigen interacts with TGF-β receptor and inhibits TGF-β signaling in colorectal cancers. Cancer research. 2010:0008-5472. CAN-10-1073.
65. Beauchemin N, Arabzadeh A. Carcinoembryonic antigen-related cell adhesion molecules (CEACAMs) in cancer progression and metastasis. Cancer and Metastasis Reviews. 2013;32(3-4):643-71.
66. Verberne CJ, Zhan Z, van den Heuvel E, Grossmann I, Doornbos PM, Havenga K, et al. Intensified follow-up in colorectal cancer patients using frequent Carcino-Embryonic Antigen (CEA) measurements and CEA-triggered imaging: Results of the randomized "CEAwatch" trial. Eur J Surg Oncol. 2015;41(9):1188-96.
67. Hasanzadeh M, Shadjou N, Lin Y, de la Guardia M. Nanomaterials for use in immunosensing of carcinoembryonic antigen (CEA): Recent advances. TrAC Trends in Analytical Chemistry. 2017;86:185-205.
68. Metildi CA, Kaushal S, Pu M, Messer KA, Luiken GA, Moossa AR, et al. Fluorescence-guided surgery with a fluorophore-conjugated antibody to carcinoembryonic antigen (CEA), that highlights the tumor, improves surgical resection and increases survival in orthotopic mouse models of human pancreatic cancer. Annal of Surgical Oncology. 2014;21(4):1405-11.
69. Boonstra MC, Tolner B, Schaafsma BE, Boogerd LS, Prevoo HA, Bhavsar G, et al. Preclinical evaluation of a novel CEA-targeting near-infrared fluorescent tracer delineating colorectal and pancreatic tumors. International journal of cancer. 2015;137(8):1910-20.
70. Wu AM. Engineered antibodies for molecular imaging of cancer. Methods. 2014;65(1):139-47.
71. Rodgers KR, Chou RC. Therapeutic monoclonal antibodies and derivatives: Historical perspectives and future directions. Biotechnology Advances. 2016;34(6):1149-58.
72. Tiernan JP, Ingram N, Marston G, Perry SL, Rushworth JV, Coletta PL, et al. CEA-targeted nanoparticles allow specific in vivo fluorescent imaging of colorectal cancer models. Nanomedicine. 2015;10(8):1223-31.
73. Kenanova V, Olafsen T, Crow DM, Sundaresan G, Subbarayan M, Carter NH, et al. Tailoring the pharmacokinetics and positron emission tomography imaging properties of anti–carcinoembryonic antigen single-chain Fv-Fc antibody fragments. Cancer research. 2005;65(2):622-31.
74. Gutowski M, Framery B, Boonstra MC, Garambois V, Quenet F, Dumas K, et al. SGM-101: An innovative near-infrared dye-antibody conjugate that targets CEA for fluorescence-guided surgery. Surgical Oncology. 2017;26(2):153-62.
75. Lutje S, Franssen GM, Sharkey RM, Laverman P, Rossi EA, Goldenberg DM, et al. Anti-CEA antibody fragments labeled with [(18)F]AlF for PET imaging of CEA-expressing tumors. Bioconjugate Chemistry. 2014;25(2):335-41.

76. Vigor KL, Kyrtatos PG, Minogue S, Al-Jamal KT, Kogelberg H, Tolner B, et al. Nanopartides functionalised with recombinant single chain Fv antibody fragments (scFv) for the magnetic resonance imaging of cancer cells. Biomaterials. 2010;31(6):1307-15.
77. da Paz MC, Santos Mde F, Santos CM, da Silva SW, de Souza LB, Lima EC, et al. Anti-CEA loaded maghemite nanoparticles as a theragnostic device for colorectal cancer. International Journal of Nanomedicine. 2012;7:5271-82.
78. Zhong Z, Wu W, Wang D, Wang D, Shan J, Qing Y, et al. Nanogold-enwrapped graphene nanocomposites as trace labels for sensitivity enhancement of electrochemical immunosensors in clinical immunoassays: Carcinoembryonic antigen as a model. Biosensensors and Bioelectronics. 2010;25(10):2379-83.
79. Huang K-W, Chieh J-J, Lin I-T, Horng H-E, Yang H-C, Hong C-Y. Anti-CEA-functionalized superparamagnetic iron oxide nanoparticles for examining colorectal tumors in vivo. Nanoscale research letters. 2013;8(1):413.
80. Hu C-MJ, Kaushal S, Cao HST, Aryal S, Sartor M, Esener S, et al. Half-antibody functionalized lipid− polymer hybrid nanoparticles for targeted drug delivery to carcinoembryonic antigen presenting pancreatic cancer cells. Molecular pharmaceutics. 2010;7(3):914-20.
81. Almeida A, Silva D, Gonçalves V, Sarmento B. Synthesis and characterization of chitosan-grafted-polycaprolactone micelles for modulate intestinal paclitaxel delivery. Drug delivery and translational research. 2017:1-11.
82. Gomes MJ, Fernandes C, Martins S, Borges F, Sarmento B. Tailoring Lipid and Polymeric Nanoparticles as siRNA Carriers towards the Blood-Brain Barrier–from Targeting to Safe Administration. Journal of Neuroimmune Pharmacology. 2017;12(1):107-19.
83. Moura CC, Segundo MA, das Neves J, Reis S, Sarmento B. Co-association of methotrexate and SPIONs into anti-CD64 antibody-conjugated PLGA nanoparticles for theranostic application. International journal of nanomedicine. 2014;9:4911.
84. Silva DS, Almeida A, Prezotti F, Cury B, Campana-Filho SP, Sarmento B. Synthesis and characterization of 3, 6-O, O'-dimyristoyl chitosan micelles for oral delivery of paclitaxel. Colloids and Surfaces B: Biointerfaces. 2017;152:220-8.
85. Patel VR, Agrawal Y. Nanosuspension: An approach to enhance solubility of drugs. Journal of advanced pharmaceutical technology & research. 2011;2(2):81.
86. Kouchakzadeh H, Shojaosadati SA, Maghsoudi A, Farahani EV. Optimization of PEGylation conditions for BSA nanoparticles using response surface methodology. Aaps Pharmscitech. 2010;11(3):1206-11.
87. Bhattacharjee S. DLS and zeta potential - What they are and what they are not? Journal of Control Release. 2016;235:337-51.
88. Di Marco M, Shamsuddin S, Razak KA, Aziz AA, Devaux C, Borghi E, et al. Overview of the main methods used to combine proteins with nanosystems: absorption, bioconjugation, and encapsulation. International journal of nanomedicine. 2010;5:37.
89. Weber C, Reiss S, Langer K. Preparation of surface modified protein nanopartides by introduction of sulfhydryl groups. International journal of pharmaceutics. 2000;211(1):67-78.
90. Xu Q, Nakajima M, Ichikawa S, Nakamura N, Roy P, Okadome H, et al. Effects of surfactant and electrolyte concentrations on bubble formation and stabilization. Journal of Colloid and Interface science. 2009;332(1):208-14.
91. Verma A, Stellacci F. Effect of surface properties on nanoparticle–cell interactions. Small. 2010;6(1):12-21.
92. Fonseca C, Simoes S, Gaspar R. Paclitaxel-loaded PLGA nanoparticles: preparation, physicochemical characterization and in vitro anti-tumoral activity. Journal of Controlled Release. 2002;83(2):273-86.
93. Kilfoyle BE, Sheihet L, Zhang Z, Laohoo M, Kohn J, Michniak-Kohn BB. Development of paclitaxel-TyroSpheres for topical skin treatment. Journal of Controlled Release. 2012;163(1):18-24.

94. Koziara JM, Lockman PR, Allen DD, Mumper RJ. Paclitaxel nanoparticles for the potential treatment of brain tumors. Journal of controlled release. 2004;99(2):259-69.
95. Zhang C, Qineng P, Zhang H. Self-assembly and characterization of paclitaxel-loaded N-octyl-O-sulfate chitosan micellar system. Colloids and Surfaces B: Biointerfaces. 2004;39(1):69-75.
96. Kim B-S, Kim C-S, Lee K-M. The intracellular uptake ability of chitosan-coated Poly (D, L-lactideco-glycolide) nanoparticles. Archives of pharmacal research. 2008;31(8):1050-4.
97. Cao Z, Ma Y, Yue X, Li S, Dai Z, Kikuchi J. Stabilized liposomal nanohybrid cerasomes for drug delivery applications. Chemical Communications. 2010;46(29):5265-7.
98. Koocheki S, Madaeni S, Niroomandi P. Development of an enhanced formulation for delivering sustained release of buprenorphine hydrochloride. Saudi Pharmaceutical Journal. 2011;19(4):255-62.
99. Thorek DL, Elias eR, Tsourkas A. Comparative analysis of nanoparticle-antibody conjugations: carbodiimide versus click chemistry. Molecular imaging. 2009;8(4):7290.2009. 00021.
100. Shen H, Jawaid AM, Snee PT. Poly (ethylene glycol) carbodiimide coupling reagents for the biological and chemical functionalization of water-soluble nanoparticles. Acs Nano. 2009;3(4):915-23.
101. Sanna V, Siddiqui IA, Sechi M, Mukhtar H. Resveratrol-Loaded Nanoparticles Based on Poly (epsilon-caprolactone) and Poly (d, l-lactic-co-glycolic acid)–Poly (ethylene glycol) Blend for Prostate Cancer Treatment. Molecular pharmaceutics. 2013;10(10):3871-81.
102. Chen K, Long DS, Lute SC, Levy MJ, Brorson KA, Keire DA. Simple NMR methods for evaluating higher order structures of monoclonal antibody therapeutics with quinary structure. Journal of Pharmaceutical and Biomedical Analysis. 2016;128(Supplement C):398-407.
103. Scott CJ, Marouf WM, Quinn DJ, Buick RJ, Orr SJ, Donnelly RF, et al. Immunocolloidal Targeting of the Endocytotic Siglec-7 Receptor Using Peripheral Attachment of Siglec-7 Antibodies to Poly(Lactide-co-Glycolide) Nanoparticles. Pharmaceutical Research. 2008;25(1):135-46.
104. Gerlier D, Thomasset N. Use of MTT colorimetric assay to measure cell activation. Journal of immunological methods. 1986;94(1-2):57-63.
105. Liebmann J, Cook J, Lipschultz C, Teague D, Fisher J, Mitchell J. Cytotoxic studies of paclitaxel (Taxol®) in human tumour cell lines. British journal of cancer. 1993;68(6):1104-9.
106. Rahman M, Laurent S, Tawil N, Yahia LH, Mahmoudi M. Nanoparticle and protein corona. Protein-nanoparticle interactions: Springer; 2013. p. 21-44.
107. Wang C-H, Huang Y-F, Yeh C-K. Aptamer-conjugated nanobubbles for targeted ultrasound molecular imaging. Langmuir. 2011;27(11):6971-6.